



MSU Graduate Theses

Spring 2022


Further Investigation of the Initiating Mechanism of the Type I Collagen Glomerulopathy

Matthew James Freese

Missouri State University, James138@live.missouristate.edu

As with any intellectual project, the content and views expressed in this thesis may be considered objectionable by some readers. However, this student-scholar's work has been judged to have academic value by the student's thesis committee members trained in the discipline. The content and views expressed in this thesis are those of the student-scholar and are not endorsed by Missouri State University, its Graduate College, or its employees.

Follow this and additional works at: <https://bearworks.missouristate.edu/theses>

 Part of the [Cell Biology Commons](#), and the [Molecular Biology Commons](#)

Recommended Citation

Freese, Matthew James, "Further Investigation of the Initiating Mechanism of the Type I Collagen Glomerulopathy" (2022). *MSU Graduate Theses*. 3758.
<https://bearworks.missouristate.edu/theses/3758>

This article or document was made available through BearWorks, the institutional repository of Missouri State University. The work contained in it may be protected by copyright and require permission of the copyright holder for reuse or redistribution.

For more information, please contact bearworks@missouristate.edu.

**FURTHER INVESTIGATION OF THE INITIATING MECHANISM OF THE TYPE I
COLLAGEN GLOMERULOPATHY**

A Master's Thesis

Presented to

The Graduate College of
Missouri State University

In Partial Fulfillment

Of the Requirements for the Degree

Master of Science, Cell and Molecular Biology

By

Matthew Freese

May 2022

Copyright 2022 by Matthew Freese

FURTHER INVESTIGATION OF THE INITIATING MECHANISM OF THE TYPE I COLLAGEN GLOMERULOPATHY

Biomedical Sciences

Missouri State University, May 2022

Master of Science

Matthew Freese

ABSTRACT

The progressive accumulation of collagen and other extracellular matrix proteins in the renal mesangium results in fibrosis, glomerulosclerosis, and eventual renal failure. Mice deficient in integrating $\alpha 2(I)$ collagen into the type I collagen structure, termed *Colla2*-deficient mice, model kidney fibrosis through the condition Type I Collagen Glomerulopathy, because homotrimeric type I collagen accumulates extracellularly in the mesangium of renal glomeruli. Accumulation of homotrimeric type I collagen compresses blood vessels in glomeruli, which reduces filtration, increases pressure, and results in fibrosis. Picrosirius red (PSR) staining was used on *Colla2* deficient and wildtype mice to evaluate collagen deposition. Histological evaluation and lesion scoring of kidney sections demonstrates that in comparison to wild-type mice, *Colla2*-deficient homozygous mice exhibit abnormal glomerular collagen deposition. Immunohistochemistry (IHC) was then used to explore initiating factors of the Type I Collagen Glomerulopathy in *Colla2* deficient and healthy mice. Platelet-derived growth factors (PDGFs) contribute to wound healing, differentiating blood and vascular tissues, repairing blood vessels, and growth of mesenchymal cells. PDGF isoforms are commonly involved in fibrosis, especially in kidneys. Using IHC, PDGF-B and PDGF-D were used to explore a relationship between Type I Collagen Glomerulopathy and these isoforms. PDGF-B was found in glomeruli and tubules of diseased tissues, while PDGF-D was only found in tubules of diseased kidneys. This relationship between PDGF-B and glomerulopathy could lead to therapeutic developments to block the deposition of collagen and limit the progression of conditions that result in renal fibrosis.

KEYWORDS: collagen, extracellular matrix, fibrosis, homotrimeric, Type I Collagen Glomerulopathy, platelet-derived growth factor

**FURTHER INVESTIGATION OF THE INITIATING MECHANISM OF THE TYPE I
COLLAGEN GLOMERULOPATHY**

By

Matthew Freese

A Master's Thesis
Submitted to the Graduate College
Of Missouri State University
In Partial Fulfillment of the Requirements
For the Degree of Master of Science, Cell and Molecular Biology

May 2022

Approved:

Amanda Brodeur M.D., Ph.D., Thesis Committee Chair

Amy Hulme, Ph.D., Committee Member

Richard Garrad, Ph.D., Committee Member

Julie Masterson, Ph.D., Dean of Graduate College

In the interest of academic freedom and the principle of free speech, approval of this thesis indicates the format is acceptable and meets the academic criteria for the discipline as determined by the faculty that constitute the thesis committee. The content and views expressed in this thesis are those of the student-scholar and are not endorsed by Missouri State University, its Graduate College, or its employees.

ACKNOWLEDGEMENTS

I would like to thank my committee members, Dr. Amy Hulme and Dr. Richard Garrad, for their help throughout my time at Missouri State. I would also like to thank my Graduate College advisor, Dr. Scott Zimmerman. A special thanks to Dr. Amanda Brodeur, who has helped me in so many ways through all 6 of my years at Missouri State.

I would also like to thank all the current and past members of my research team: Kaitlyn Armstrong, Drake Headrick, Grant Headrick, Olivia Hetzel, Rachel Ingram, Travis Jackson, Garrett Reid, Clare Scheier, Kambria Todd, Lillian van Biljon, Kaitlyn Weber, and Peyton Wombacher.

I would also like to thank my family for their incredible support through my schooling. Also, a huge thank you to my amazing partner, Madison.

TABLE OF CONTENTS

Background	Page 1
Clinical Significance	Page 1
Kidney Structure	Page 1
Renal Fibrosis	Page 3
Modeling Fibrosis	Page 4
Platelet-Derived Growth Factors	Page 6
Research Aims	Page 7
Methods	Page 18
Mouse Kidneys	Page 18
Processing Kidney Samples	Page 18
Sectioning Kidney Samples	Page 19
Picosirius Red Staining Slides	Page 20
Visualizing and Lesion/Morphometry Scoring Slides	Page 21
Immunohistochemistry of PDGF-B and PDGF-D	Page 22
Visualizing and Assessing PDGF Presence	Page 26
Verifying Disease State and Lesion Scores Of Genotypes	Page 28
Determining Differential Presence of PDGF-B and PDGF-D	Page 36
Discussion	Page 44
References	Page 47

LIST OF TABLES

Table 1. Mouse Identification Sheet	Page 27
Table 2. Assigned Lesion Scores Following PSR	Page 32

LIST OF FIGURES

Figure 1. Macroscopic Structure of Kidney	Page 11
Figure 2. Microscopic Structure of Kidney and Nephron	Page 12
Figure 3. Blood Flow to Glomeruli of Kidney	Page 13
Figure 4. Glomerular Structure and Cell Types	Page 14
Figure 5. Comparison of Heterotrimeric and Homotrimeric Type I Collagen Isotypes	Page 15
Figure 6. Comparison of Heterotrimer and Homotrimeric Type I Collagen in Fibril	Page 16
Figure 7. PDGF Dimer Isoforms and Binding	Page 17
Figure 8. PSR Internal Control Vessels	Page 33
Figure 9. PSR Lesion Score Representative Images	Page 34
Figure 10. PSR Comparison	Page 35
Figure 11. IHC Controls	Page 40
Figure 12. IHC with PDGF-B	Page 41
Figure 13. IHC with PDGF-D	Page 42
Figure 14. IHC Comparison Between PDGF Monomers	Page 43

BACKGROUND

Clinical Significance

Chronic Kidney Disease (CKD) is a condition in which kidneys become progressively more damaged. Because the kidneys are not able to filter blood as effectively, waste accumulates which can eventually lead to renal failure. Kidney diseases can lead to anemia, heart disease, edemas, weak bones, a weakened immune system, and eventually death.¹ Kidney diseases affect 37 million Americans or 15%, with many of those being undiagnosed.² Risk factors for developing CKD include hypertension, diabetes, heart disease, smoking, and old age.^{2,3} Diet and lifestyle changes can limit the progression of early CKD, and dialysis and kidney transplants can treat late-stage renal failure. Understanding the progression of kidney diseases can lead to better therapies to ease symptoms and slow development. Previous research has shown that collagen deposition in glomeruli and mesangial matrix expansion are both elements of kidney diseases.^{4,5}

Kidney Structure

Kidneys filter blood from the body. The kidney is surrounded in a protective cortex, which makes the border around the renal medullas. Within a kidney, there are typically 6-12 medullas, which are the functional areas of the kidney. Medulla are divided into smaller renal pyramids, containing many small tubule structures called nephrons. Nephrons are considered the functional unit of the kidney, as they are where filtration, secretion, and reabsorption of products from the blood occurs. The site of filtration within a nephron is a glomerulus, which is a bundle of capillaries surrounded by a glomerular capsule. Figure 1 below shows the macroscopic structure of a kidney as well as their anatomical placement in the human body. Figure 2 below shows the structure of a nephron, where filtration, reabsorption, and secretion occur to synthesize urine.⁶ The glomerulus will

filter blood, storing urine in the urinary space. Following the filtration that occurs in the glomerular tubules, the rest of urine production occurs in the proximal and distal tubules, which are a singular branch off from the glomeruli. The proximal convoluted tubule is primary site of reabsorption, in which glucose, water, peptides, and electrolytes are pushed back into the bloodstream from the tubule. This resorptive action continues in the proximal straight tubule/thick descending loop of Henle. The byproduct of the process is urine, which is passed into the ureters to the bladder.⁶

Blood enters the kidney through the renal artery, which branches into five segmental arteries, which further branch into additional arteries before they eventually become afferent arterioles which will flow into individual glomeruli. When blood reaches the nephron, filtration will begin. Figure 3 below shows the structure of the renal artery and its divisions into the various branches to reach a glomerulus.^{7,8}

Glomeruli are the first segment of the nephron. Filtration of blood occurs in the glomerulus, where urine is pushed into the urinary space of each glomerulus. Several tissues make up the glomerulus: mesangial cells, parietal epithelial cells, podocytes, endothelial cells, and tubular epithelial cells.⁹ These cell types and the structures they form are shown in Figure 4 below.⁹ Mesangial cells make up the connective center of the glomerulus, and are 30-40% of the total cells in the glomerulus.¹⁰ These cells are very important for maintaining the structure of glomeruli and holding the capillaries in place.¹¹ The mesangial matrix is the branching tissues that lead from afferent arteries into the glomeruli of renal medullas. Epithelial cells line the capsule and capillaries within the glomeruli. Two kinds of epithelial cells are present in glomeruli: parietal epithelial cells, which form the glomerular capsule, and podocytes that sit on the external surface of glomerular capillaries. Tubular cells are the final cell type in glomeruli. They make up the internal lining of the glomerular capillaries.¹² Another important structure within glomeruli is the urinary space, which is a

gap between the glomerular capillaries and the parietal layer of the glomerular capsule. When collagen is deposited in the mesangium of glomeruli, this space is often reduced or eliminated, eventually resulting in decreased glomerular filtration.

Renal Fibrosis

Renal fibrosis, which is characterized by the progressive accumulation of type I collagen and other proteins in the extracellular matrix of the mesangium of glomeruli, is a symptom involved in many kidney pathologies.¹³ Renal fibrosis is a target for therapeutic interventions in treating many conditions and diseases. Some long-term conditions lead to the slow development of renal fibrosis, including diabetes, hypertension, and obesity. Other short-term conditions lead to rapid development of renal fibrosis, including Acute Kidney Injury/Acute Renal Failure (AKI/ARF) and ureteral obstruction. Renal fibrosis can be detrimental, as it can lead to continual accumulation of waste such as urea, metabolic byproducts, salts and water in the kidneys, eventually resulting in renal failure, sepsis, and death.

Renal fibrosis typically begins from a minor increase in hydrostatic pressure in the mesangium from hypertension, injury, or high blood sugar. Hydrostatic pressure is essential in kidneys to force fluid through nephrons. When there is obstruction to the vessels fluid flows through, hydrostatic pressure increases to maintain flow. The increase in hydrostatic pressure results in tissue damage, cell death, and finally connective tissue proteins such as collagen I, collagen III, and fibronectin replacing the damaged tissues. The proteins often prevent functionality of those areas of the kidney, resulting in continual increases in hydrostatic pressure, further damage, and increased accumulation of extracellular proteins. Over time, progressive accumulation of proteins in the mesangium results in decreased flow of blood into glomeruli, which reduces the rate in which

glomeruli can process blood, lowering filtration rate. This lowered filtration rate can be measured to estimate kidney functionality, which is termed glomerular filtration rate (GFR). GFR is a measure of the amount of blood passing through glomeruli in a minute. As glomeruli accumulate tissue damage, less blood is filtered, resulting in a lowered GFR. Continued reduction of filtration results in continual damage to glomeruli, resulting in decreased urine production and increased waste in the kidneys.⁶

Modeling Fibrosis

While renal fibrosis often takes years to develop in humans, it can be modeled in rodents quickly by using more acute sources of renal damage. There are several ways to cause fibrosis, such as gene alterations, blockages, or induced infections.¹⁴

Rodents are a model organism used to study various physiological conditions. Mice are particularly useful for studying renal function, because of their developmental similarities to humans. Similar to humans, mouse kidneys develop many glomeruli in utero, but not all are immediately functional. Glomeruli of mice become functional after about 21 days. Mice are also useful models for kidney function because renal pathologies can be induced in mice to inform researchers about the conditions in humans.¹³

Osteogenesis imperfecta (OI) is a disease involving the abnormal formation of type I collagen in bones, resulting in curved spines, brittle bones, severe skeletal fragility, osteopenia, and skeletal deformity.¹⁵ The osteogenesis imperfecta mouse model (*oim*) is a valuable model for several pathologies. These mice produce exclusively homotrimeric type I collagen, because of an inability to integrate $\alpha(2)$ collagen chains into the final collagen I protein structure due to its rapid degradation.¹⁶ *Oim* are also referred to as *Colla2*-deficient mice because of their disease state. Initially, this

mutation was used to study osteogenesis imperfecta, which causes defects in the musculoskeletal system of the model mice. The homozygous *oim* mice are considered to have moderately severe OI, with reduced bone density and fragility. This condition is analogous to the rare autosomal recessive form of OI found in humans. Other systems besides the musculoskeletal system were evaluated in these mice, which determined that all tissues were wildtype except the kidneys.¹⁵ The kidneys show significant lesions, type I collagen deposition in glomeruli, and expanded mesangia, but no alteration to basement membranes or vessels outside the kidney.¹⁵ These mice also develop chronic glomerulopathy, a disease of renal glomeruli, causing reduced glomerular filtration. Chronic glomerulopathy can be used as a model to study renal diseases.¹⁵ Research also involves heterozygous mice, with one wildtype allele and one *Colla2* deficient allele. Initially, heterozygous mice were categorized as having no lesions, although it was later determined they exhibit less severe lesions than *Colla2*-deficient mice.

Normal type I collagen is heterotrimeric, being comprised of two $\alpha 1(I)$ monomer chains and one $\alpha 2(I)$ monomer chain. These three chains wrap together to form a triple helix. Homotrimeric collagen is instead comprised of three $\alpha 1(I)$ chains. Although pathogenic in high quantities, homotrimeric collagen is also found in adult skin in low levels, in embryonic development, and during wound healing. The homotrimeric collagen is also referred to as *Colla2*-deficient, because it lacks the $\alpha 2(I)$ chain that is present in heterotrimeric collagen I. Because of the homotrimeric nature of the *Colla2*-deficient collagen, fibril assembly is disrupted which results in thicker, disorganized, and less dense collagen I fibrils. In the extracellular matrix of renal glomeruli, homotrimeric type I collagen accumulates, which compresses blood vessels due to their thicker shape. The increased pressure from compressed blood vessels leads to damage and fibrotic tissue aggregating in the mesangium of glomeruli. Figure 5 below shows the fibrils involved in each isotype of type I

collagen. Figure 6 below shows how the improperly shaped fibrils of homotrimeric type I collagen result in pathologic accumulation.¹⁷

Platelet-Derived Growth Factors

Previous research has shown that neither transforming growth factor beta 1 (TGF- β) nor tumor necrosis factor alpha (TNF- α) show significant presence in Type I Collagen Glomerulopathy, decreasing their potential as initiators of renal fibrosis.¹⁸ Both of these factors were found to be independent of fibrosis via immunohistochemistry (IHC), which assessed whether the factors were related to fibrotic factors or glomerulopathy.

With these two potential initiators ruled out, the focus turned to platelet derived growth factors (PDGFs). These factors derive from platelets, which are small cells in the blood and clot at sites of tissue injury. Platelets minimize blood loss following tissue damage. PDGFs contribute to wound healing, blood vessel development, and blood vessel restoration.¹⁹ Because of the characterization of fibrosis including swelling and destruction of blood vessels, PDGFs are likely involved in initiating collagen I deposition to replace damaged tissue in the mesangium of renal medulla.

PDGFs come from four genes and create five dimers, as shown in Figure 7 below.²⁰ The four PDGF genes are PDGF-A, PDGF-B, PDGF-C, and PDGF-D. The five dimers are a combination of the resulting proteins from each gene, resulting in dimers AA, AB, BB, CC, and DD. These dimers interact with two different receptors, called platelet-derived growth factor receptors (PDGFR).²¹

The receptors are also formed from dimers, which originate from two genes: PDGFR- α and PDGFR- β . The two most common receptor dimers are PDGFR- $\alpha\alpha$ and PDGFR- $\beta\beta$. PDGFR- $\alpha\alpha$

is activated by PDGF types; AA, BB, AB, and CC. PDGFR- $\beta\beta$ is activated by PDGF types BB and DD. There is a less common receptor dimer that comes from one monomer from each gene: PDGFR- $\alpha\beta$. This receptor has low affinity for most PDGF dimers, but research and understanding of this receptor dimer is limited.¹⁹

PDGF-BB dimer was chosen for this research because of its versatility in all three receptor types (PDGFR- $\alpha\alpha$, PDGFR- $\beta\beta$, and PDGFR- $\alpha\beta$). The PDGF-B monomer is also involved forming two isomers of PDGF (PDGF-AB and PDGF-BB). The versatility of the PDGF-B monomer and the PDGF-BB dimer could increase its likelihood of being an initiator in fibrosis pathways. PDGF-DD also primarily binds PDGFR- $\beta\beta$, although it has a low affinity for PDGFR- $\alpha\beta$. PDGF-BB and PDGF-DD have been consistently associated with fibrosis in multiple organ tissues, including renal, cardiac, and hepatic. PDGF-CC is also a candidate for initiation of fibrosis in renal tissues, but it is not compatible with IHC protocols because there are no antibodies developed for the procedure. Also, PDGF-CC binds PDGFR- $\alpha\alpha$, which has slightly different traits. PDGFR- $\alpha\alpha$ can be indirectly activated by molecules other than PDGFs. However, PDGFR- $\beta\beta$ can only be directly activated by one of its specific PDGF isoforms. Thus, this research focuses on confirming the disease state and symptoms in the kidney samples, then using IHC to show association and initiation of fibrosis by PDGF-B and PDGF-D.¹⁸⁻²¹

Research Aims

Lesion Score Wildtype, Heterozygous, and *Colla2* Deficient Mice. In this research, PSR and Lesion/Morphometry Scoring will be performed on wildtype, heterozygous, and *Colla2*-deficient mouse kidney sections to verify that the Type I Collagen Glomerulopathy model and the specific mice in this lab are viable for studying renal fibrosis. The PSR stain should bind to the type I

collagen in the kidney samples, staining them orange or red. In a healthy state, collagen I is sparse in a healthy kidney, with collagen IV and V comprising the largest portion. However, collagen I is found in high prevalence in severe disease states, with collagen III also being present. Thus, Picrosirius red staining (PSR) is an important step in analyzing models for diseased kidneys. Under polarized light, PSR stains all collagen red, collagen I yellow, and collagen III green. With the type I and type III staining differently than other collagens, the proportion of pathogenic collagen can be determined to confirm the disease state. These specific stains for collagen make PSR a very valuable method for viewing fibrosis, as type I and III collagen are two of the main extracellular matrix proteins that contribute to fibrosis.

It is expected that the glomeruli of the wildtype kidney samples should show minimal red staining within the glomeruli, because they are not diseased. Wildtype mice have the ability to integrate $\alpha 2$ chains into the collagen I structure, so they will still create healthy, heterotrimeric collagen I. Thus, the wildtype glomeruli should be healthy; a contained circle, with rounded edges that do not reach the edge of the border. The glomeruli of heterozygous type I collagen glomerulopathy kidney samples should show some orange staining in the glomeruli. This small amount of staining is because heterozygous mice will have some healthy, heterotrimeric collagen I, but will additionally have some pathologic homotrimeric collagen I. The glomeruli of homozygous type I collagen glomerulopathy kidney samples should show high amounts of orange staining in the glomeruli. This high amount of orange staining is because the homozygous mice lack a healthy copy of the gene, and therefore only make homotrimeric collagen I. Both the heterozygous and homozygous type I collagen glomerulopathy samples should show stretching, distension, and deformity in the glomeruli. In a later disease state, the glomeruli may also collapse into a small pellet, indicative of significant damage that results in a nonfunctional, scarred glomeruli.

Wildtype kidney slides are expected to have lesion scores of 0, heterozygous slides are expected to have lesion scores of 1-2, and homozygous type I collagen glomerulopathy slides are expected to have lesion scores of 3-4. The higher lesion score is a result of the presence and accumulation of homotrimeric collagen I in the mesangium of glomeruli leading to damage to the glomeruli.

Assess PDGF-B Presence in Wildtype, Heterozygous, and *Colla2* Deficient Mice.

Because PDGFs are often involved in vascular damage and fibrosis, it is expected that PDGF-B will be present in high amounts in the *Colla2* deficient mouse kidney sections. However, there will likely be some PDGF-B shown in wildtype mouse kidney sections as well, because of basal expression of PDGF-B.

Performing IHC with PDGF-B will stain the monomer brown within the mouse kidney section. This staining will show where PDGF-B monomers are located within mouse kidney sections from the wildtype, heterozygous, and *Colla2*-deficient mice. Brown staining is expected especially in homozygous *Colla2* deficient mice, as they have Type I Collagen Glomerulopathy resulting in excess collagen I deposition, potentially from PDGF-B signaling. For wildtype mice, there should be limited brown staining in throughout mouse kidney sections from basal expression. Heterozygous *Colla2*/wildtype mice should show slight brown staining.

Assess PDGF-D Presence in Wildtype, Heterozygous, and *Colla2* Deficient Mice.

Similarly, because of PDGFs role in vascular damage and fibrosis, it is expected that PDGF-D will be present in high amounts in the *Colla2*-deficient mouse kidney sections. Some basal expression of PDGF-D is also expected in wildtype tissues.

Performing IHC with PDGF-D will stain the monomer brown within the mouse kidney sections. Because this is a different isoform of PDGF monomer, it is expected that there will be different amounts and potentially in different locations. However, with PDGF-D as well, *Colla2*-

deficient mice are expected to have the most brown staining, heterozygous *Colla2*-deficient/wildtype mice should show slight brown staining, and wildtype mice are expected to have only minimal, basal staining.

Comparison of PDGF-B and PDGF-D. The overall goal of the IHC is to determine if there is an increase in PDGF-B or PDGF-D in diseased kidneys compared to wildtype kidneys. Because this model of fibrosis occurs in the glomeruli, PDGFs in glomeruli of the mouse kidney samples are of particular interest. PDGF-B may overall show more presence because of its versatility. It is a component of two isoforms of PDGF (BB and AB) and has affinity for both of the most common receptor dimers ($\alpha\alpha$ and $\beta\beta$) and also shows affinity for the less common $\alpha\beta$ receptor dimer.

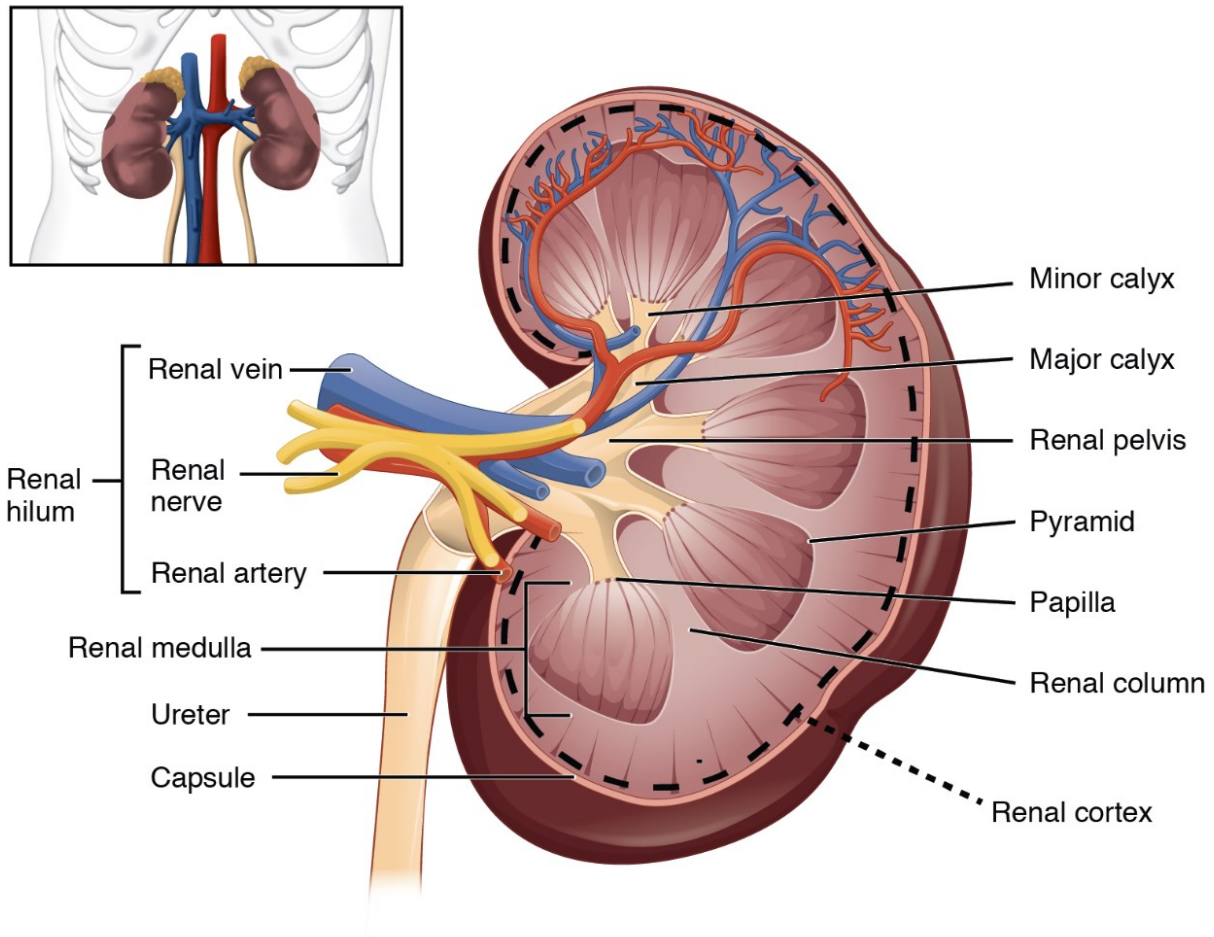


Figure 1. Macroscopic Structure of Kidney. Image shows large structure of kidney. Inlet in upper left shows anatomical location of kidneys within thoracic cavity.

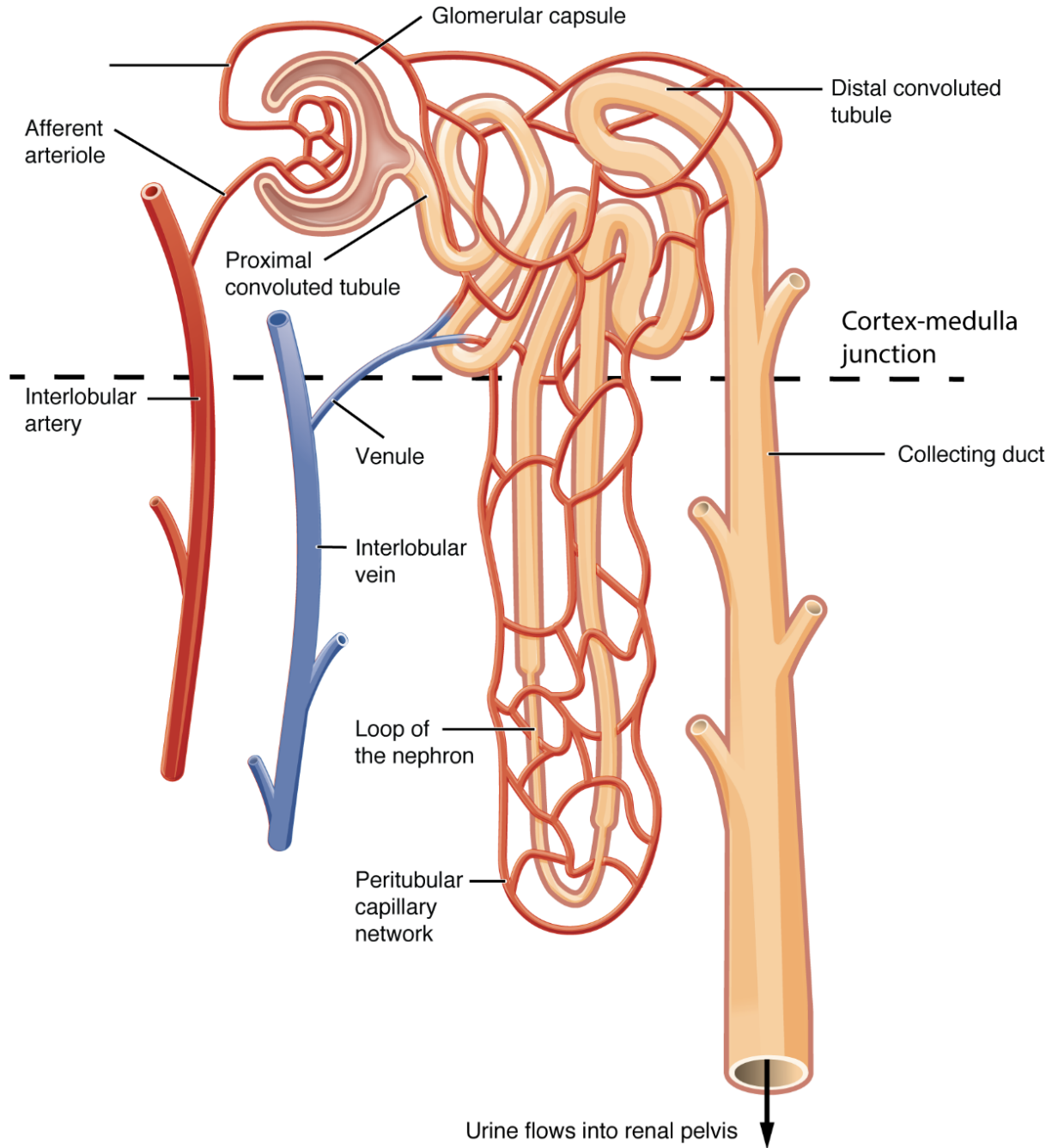


Figure 2. Microscopic Structure of Kidney and Nephron. This figure shows the smaller-scale structure of a nephron. An area of particular importance is the glomerular capsule, glomerular network within, and urinary space between them.

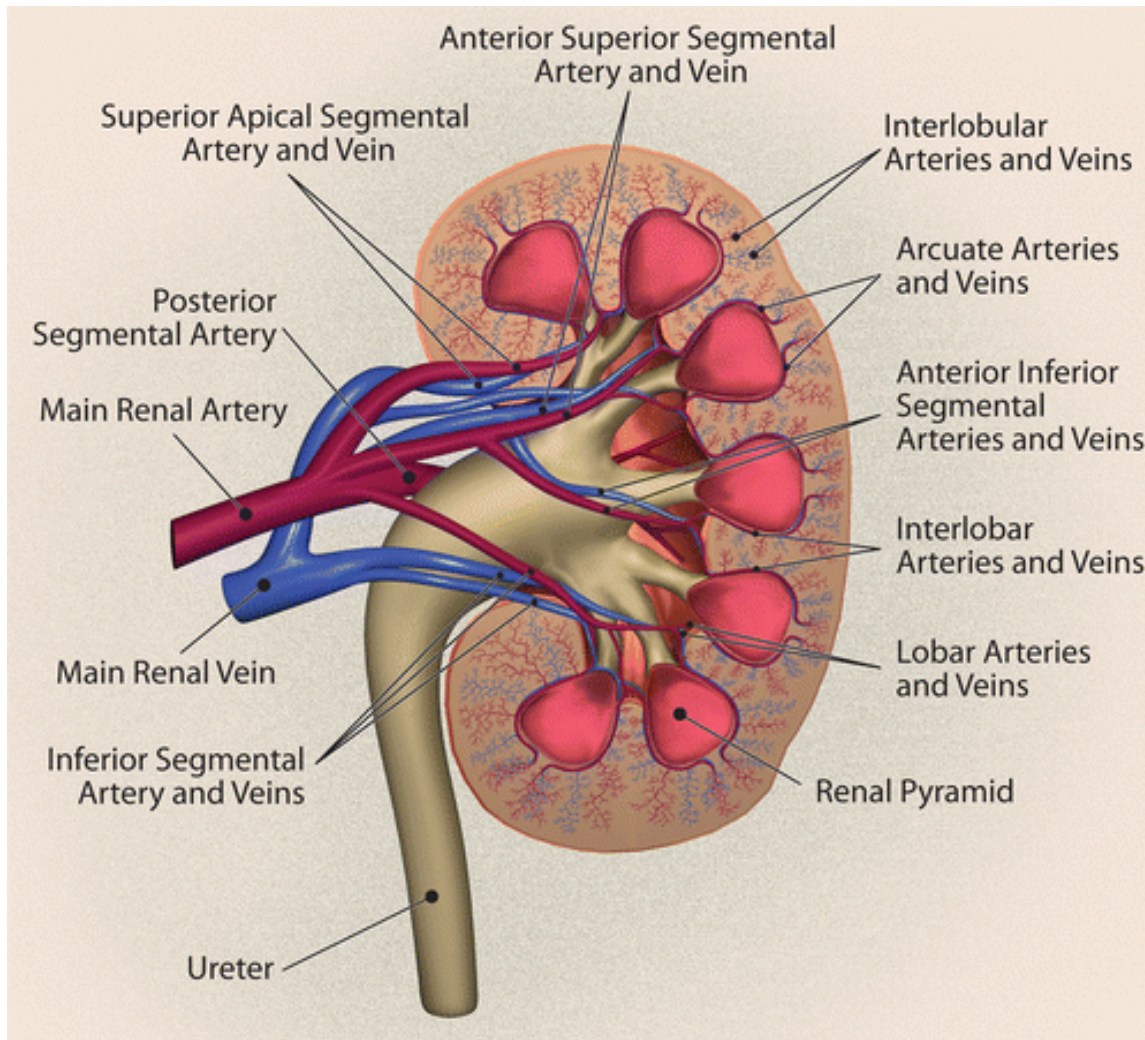


Figure 3. Blood Flow to Glomeruli of Kidney. Blood enters the kidney through the main renal artery, seen at the left side of this image. The main renal artery splits into segmental arteries, which lead to the renal pyramids. Segmental arteries branch into interlobar arteries, which travel around the periphery of renal pyramids. Interlobar arteries branch into arcuate arteries and veins. Arcuate branch into interlobular arteries, which lead into the individual glomeruli.

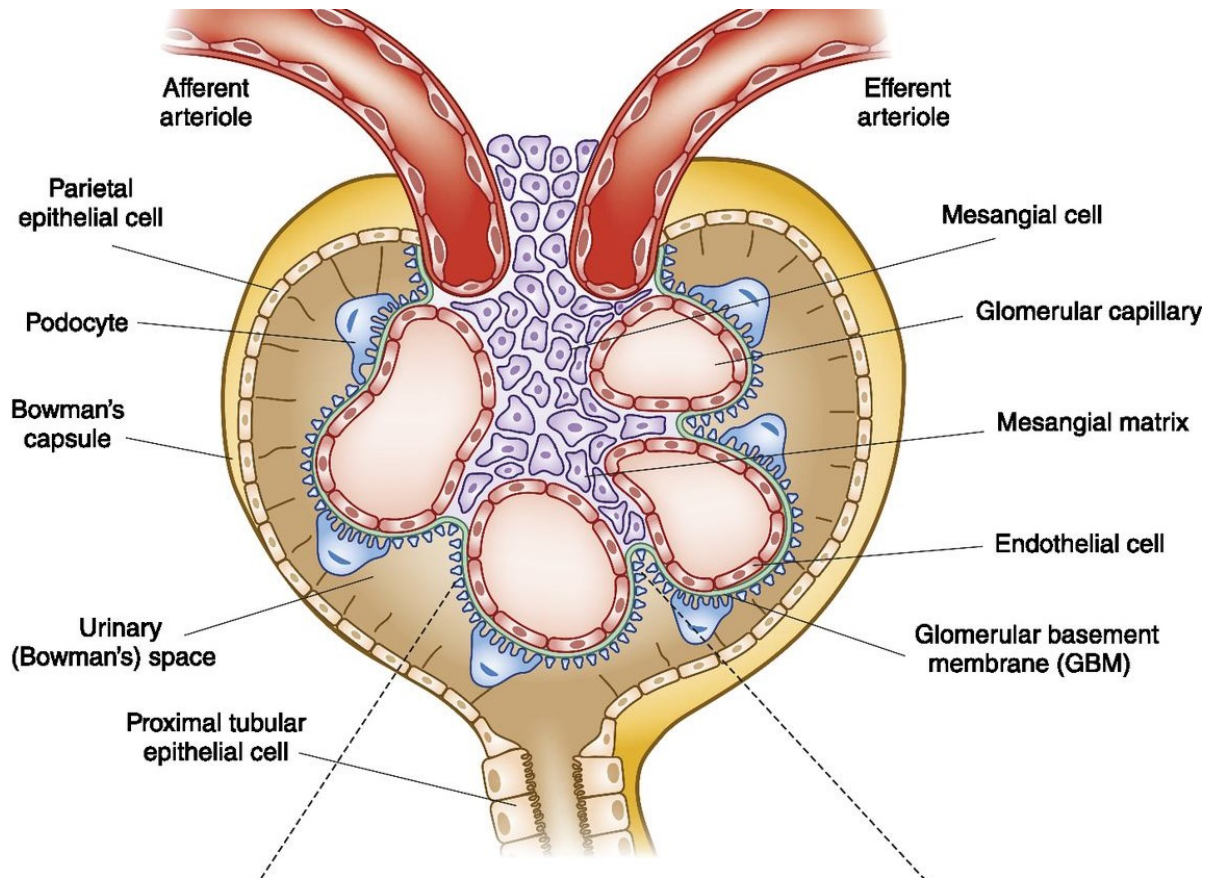
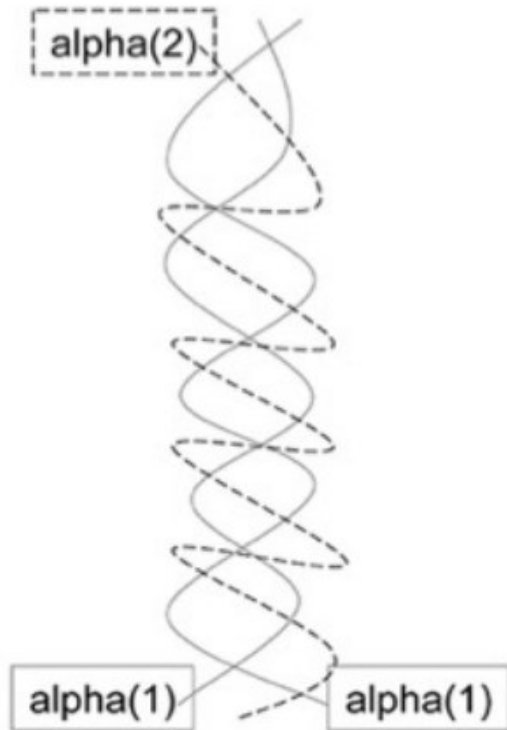


Figure 4. Glomerular Structure and Cell Types. Blood flows into glomerular capillaries from the afferent arteriole. Blood exits the glomerular capillaries through the efferent arteriole, but urine is filtered out into the urinary space, where it will continue travelling down the nephron's tubules. Many cell types are important in maintaining the glomerular structure, including the mesangial cells, podocytes, tubular epithelial cells, and parietal epithelial cells.

Heterotrimeric



Homotrimeric

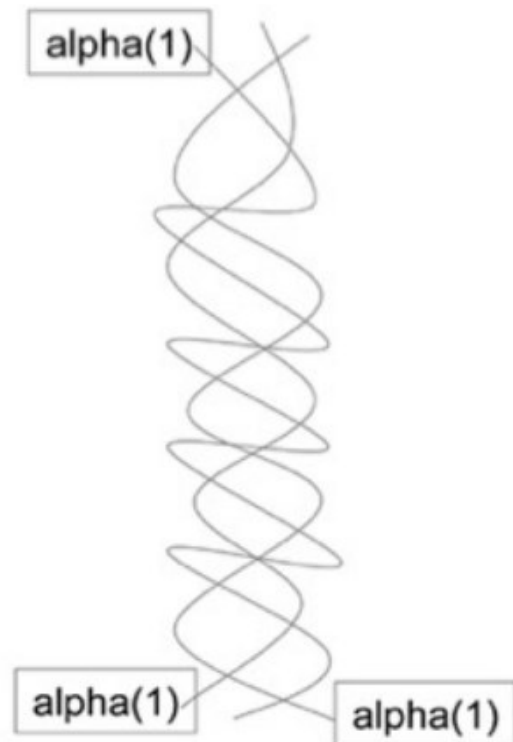


Figure 5. Comparison of Heterotrimeric and Homotrimeric Type I Collagen Isoforms. The heterotrimeric isoform is most commonly seen throughout the body. It is comprised of 2 alpha(1) chains and 1 alpha(2) chain that wrap together to form a triplehelix. The homotrimeric isoform is found in select situations, such as during wound healing and in embryological development. It is comprised of 3 alpha(1) chains that wrap into a triplehelix. Figure created by Amanda Brodeur, MD/PhD.

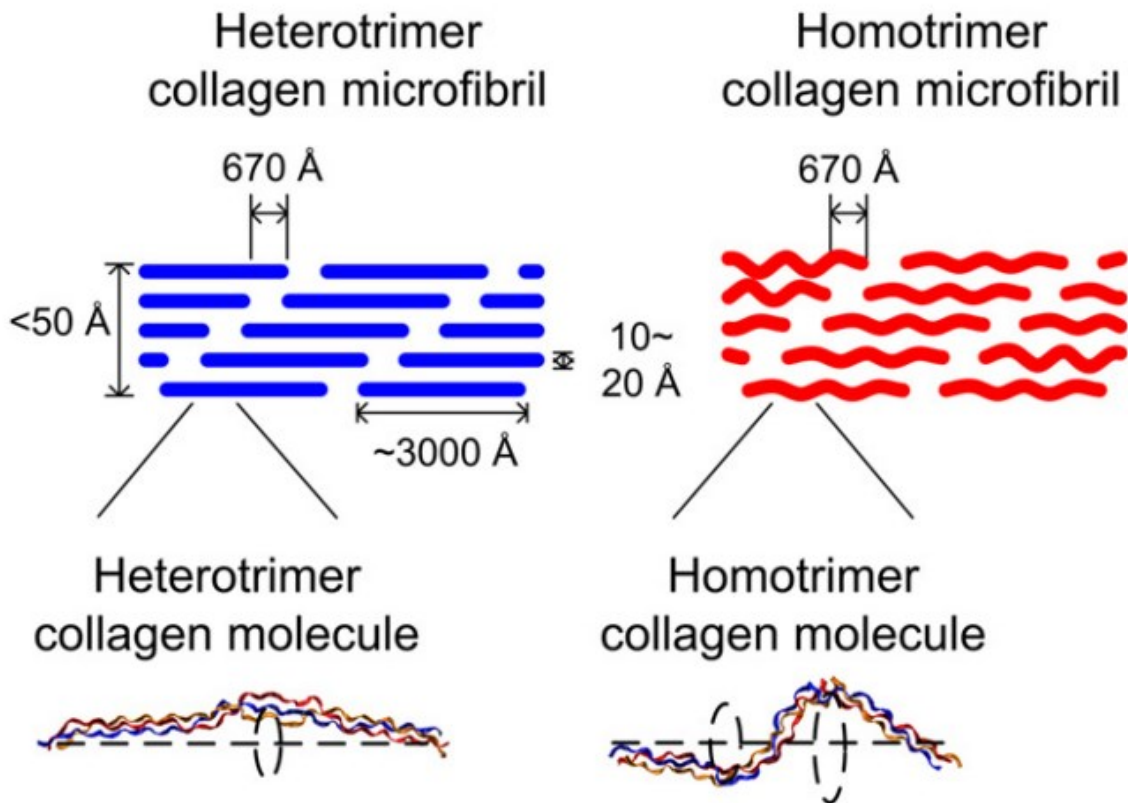


Figure 6. Comparison of Heterotrimer and Homotrimeric Type I Collagen in Fibril. On the left, heterotrimeric type I collagen form organized, straight fibrils. These fibrils are thin, causing them to stack orderly. On the right, homotrimeric type I collagen form wavy fibrils. These fibrils become much thicker, in a helical shape, causing them not to stack orderly. In the proper collagen structure on the left, binding between fibrils leads to a denser and stronger structure. However, in improper collagen structure on the right, the binding is disrupted leading to reduced strength and potential obstruction as seen in Type I Collagen Glomerulopathy.

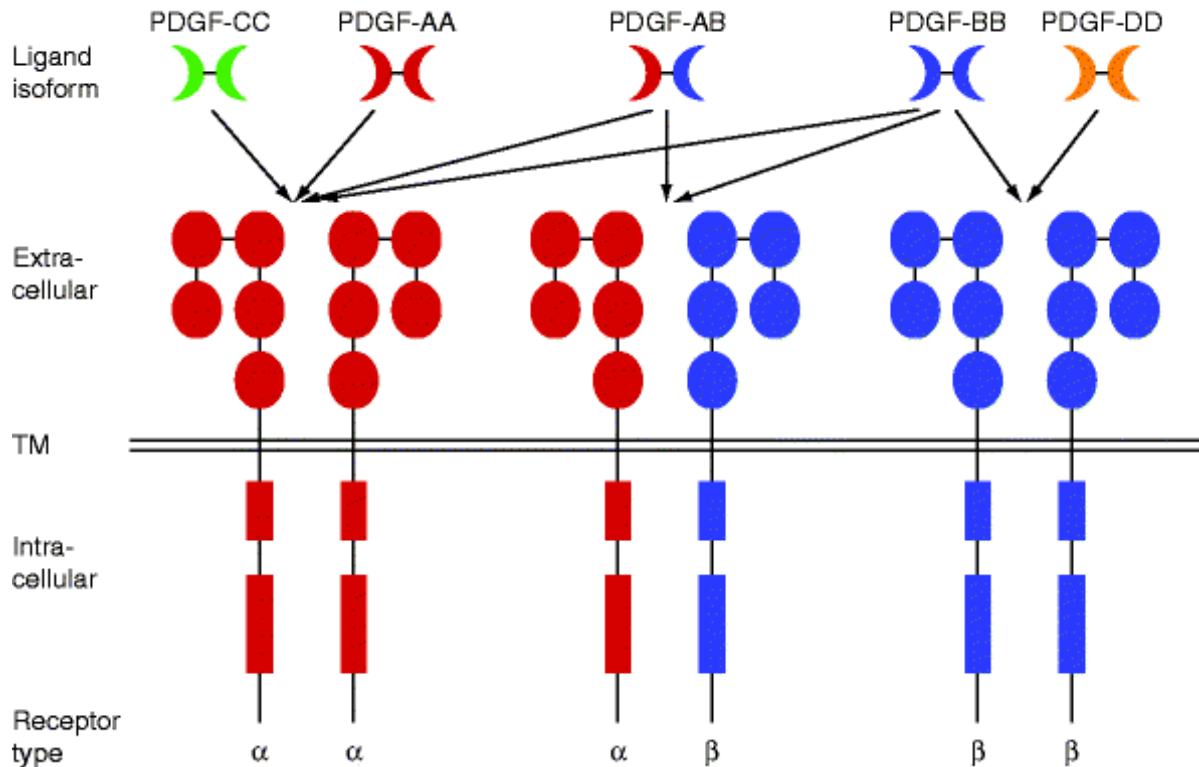


Figure 7. PDGF Dimer Isoforms and Binding. This figure summarizes the binding affinity each PDGF dimer isoform has for each PDGFR dimer isoform. Notably, PDGF-BB has affinity for all three receptor isoforms, while PDGF-DD only has affinity for PDGFR- $\beta\beta$.

METHODS

Mouse Kidneys

Mouse kidneys were obtained from University of Missouri. No mouse care was done at Missouri State University or by individuals affiliated with Missouri State University.

Heterozygous B6C3Fe a/a-*Col1a2*oim/J (*Col1a2*-deficient +/-) mice were purchased from the Jackson Laboratory (Bar Harbor, ME, USA), and bred and genotyped as previously published to generate wildtype (+/+), heterozygous (+/-), and *Col1a2*-deficient (-/-) animals. All animal care conformed to the National Institutes of Health Guide for Care and Use of Laboratory Animals and was approved by the University of Missouri Animal Care and Use Committee (an AAALAC accredited animal facility), Columbia, MO, USA (Protocol Registry Number 3579; Animal Welfare Assurance Number A3394-01). Mice were sacrificed and the kidneys were harvested. Kidneys were stored in 70% ethanol and shipped to Missouri State University.

Table 1 shows the kidney samples used in this lab as received from University of Missouri. Mice are categorized as homozygous wildtype (wt), heterozygous (het), or homozygous oim (oim). Homozygous oim mice also suffer from Type I Collagen Glomerulopathy and are used to model that condition in lab. Heterozygous mice are expected to show wildtype condition, according to University of Missouri and previous research.

Processing Kidney Samples

Using forceps, one kidney was removed from ethanol fixation and placed in a weigh boat. While stabilizing the kidney with the forceps, the kidney was cut in the longitudinal plane. One half of the kidney was placed cut side down into a blue cassette and labeled with a graphite pencil. The cassette was closed and placed into 70% ethanol.

The tissue processor (Leica ASP300S) was warmed up for 12 hours before use. Reagent bottles were checked and refilled if necessary. The cassettes were removed from the 70% ethanol and placed in the tissue processor with cassette facing up. '10-hour Overnight Program' was selected then the number of cassettes in the basket was entered and 'Yes Ready to Begin' was selected.

Prior to removing kidneys from the tissue processor, a metal tray was warmed on the hot plate at 60°C. The metal basket holding the kidney cassettes was removed from the tissue processor. The cassettes were transferred from the metal basket to a beaker, then placed in the oven. To embed, a cassette was removed from the oven and opened. A clear mold was placed onto the hot plate, the molten paraffin was removed from the oven, and then the paraffin was poured to fill the imprinted square. Using forceps, the kidney was placed into the square with the cut side down. It was then covered with the slanted and labeled side of the cassette. Enough molten paraffin was poured on top of the cassette to cover the surface. The mold with the cassette was placed on ice then once cloudy, the molds were stored at 4°C in a labeled container.

Sectioning Kidney Samples

A rotary microtome was used to section the kidney samples. The microtome was locked, and the blade was inserted. Samples were placed in the specimen holder. The blade holder base was adjusted to align with the sample, and the thickness dial was set to 5 microns. The locking lever was placed into the unlocked position, and the hand wheel was used to slide the tissue block across the blade. If the paraffin began to melt, the sample was removed and briefly placed on ice before sectioning could continue. Once the paraffin sections began containing the sample instead of only paraffin wax, the sections were carefully placed into the warm water bath. After

the wax began to melt, the samples were removed from the water by using a clean microscope slide. The slides were labeled with the sample number, genotype, and date and placed into the slide warmer for 24 hours. These steps were repeated for each sample, using a new water bath for each one. Once sectioning was completed, the locking lever was returned to the locked position, the blade was removed, and the waste tray was emptied.

Picrosirius Red Staining Slides

The procedure for PSR staining largely follows the Polysciences Picrosirius Red Stain Kit procedure with a few modifications (“Picrosirius Red Stain Kit.” *Polysciences Inc.* Catalog #24901).²²

The sectioned kidney slides were removed from the fridge, and first deparaffinized in xylene washes in staining dishes. After 3 minutes in this dish of xylene, the staining tray was removed and placed in a different dish, also filled with xylene. After 3 minutes in this second dish of xylene, the staining tray with the tissue slides was again removed and placed in a third dish, also filled with xylene.

After the xylene washes, the tissue slides were hydrated in ethanol washes in new staining dishes. The tissues were hydrated in 100% ethanol for 6 minutes (and shaken after 3 minutes), 100% ethanol for an additional 3 minutes, 95% ethanol for 1 minute, 75% ethanol for 1 minute, then deionized (DI) water for 3 minutes to rinse. In this rinse step, the staining tray was again shaken up and down to mix the water around and ensure all ethanol was rinsed off the slides.

After the ethanol hydrations and DI water rinse, the tissues were stained with the PSR solutions. The first was solution A for 2 minutes, which is phosphomolybdic acid, used to prevent the Picrosirius red from binding the nucleus nonspecifically. Following the submersion in solution A, the

staining tray with the tissue slides were rinsed in DI water for 1 minute with shaking. The next was solution B for 60 minutes, which is Picosirius red F3BA stain to stain collagen. The staining tray with the tissue slides was then rinsed in fresh DI water for 1 minute with shaking. The last was solution C for 2 minutes, which is hydrochloride acid.

Following the use of the PSR solutions, the tissue samples were dehydrated by placing them in ethanol solutions of increasing concentration. Tissue samples were hydrated in 75% ethanol for 45 seconds, 95% ethanol for 1 minute, 100% ethanol for 6 minutes (with shaking after 3 minutes), and 100% ethanol for an additional 3 minutes.

Following the dehydration, the tissue samples were removed from the staining tray and were fixed with cover slips using Permout (Fisher SP15-500). Each tissue slide is removed individually. In a beaker, solidified Permout was mixed with reused xylene until the beaker has a syrup-like consistency. A glass stir rod was placed in the beaker and 3 drops were placed on the stained tissue. A coverslip was placed over the smeared Permout and pushed down to release any bubbles. The tissue slides with the added coverslips were then left out in the fume hood overnight to dry.

Visualizing and Lesion/Morphometry Scoring Slides

Following PSR, the kidney slides were stored at room temperature. They were visualized via light microscopy to view the collagen staining, lesion score (or morphometry score), and general health of the kidney. Under the microscope, the red coloration is bound Picosirius red stain. It binds and stains type I and III collagen. Blood vessels are stained red, which are surrounded by type I collagen. These vessels should be thin, uniform uncolored strips with red borders. These function as an internal control to ensure the blood vessels are properly stained, which suggests the collagen are properly stained as well. They are 1/10 the size of a vessel and should be a small uniform circle. In

diseased mice, the circle will be stretched, wrinkled, pushing the borders of the vessel, and covered in orange collagen. The amount that glomeruli are stained orange (the amount of collagen) denotes the lesion/morphometry score, which translates to the health of the kidney.

A lesion/morphometry score of 0 means that no collagen deposition in the glomeruli, a score of 1 means there is less than 25% of the glomerular area occupied by collagen, a score of 2 means 25-50% of the glomerular area is occupied by collagen, a score of 3 means 50-75% of the glomerular area is occupied by collagen, and a score of 4 means greater than 75% of the glomerular area is occupied by collagen. The orange coloration shows that collagen occupies the glomeruli. A more diseased kidney is indicated by a higher lesion/morphometry score. The lesion/morphometry scores are used to support the genotyping of the kidney samples¹³.

Immunohistochemistry of PDGF-B and PDGF-D

The procedure for IHC largely follows the Immunoperoxidase Staining Protocol from Santa Cruz Biotechnology (“Immunoperoxidase Staining.” *Santa Cruz Biotechnology*).²³

This procedure follows processing and sectioning kidney samples. Only one stain was done for each sectioned kidney sample (either PSR or IHC). Before starting the procedure, one wildtype kidney sample was designated as the negative control/secondary antibody only treatment. This sample was not incubated in primary antibody but was still incubated with secondary antibody and chromogen. A second wildtype kidney sample was chosen (but not designated as a negative control) and received all the treatments (including primary antibody), but this sample is not expected to show specific staining. Additionally, one *Colla2* deficient sample was designated negative control/secondary antibody only treatment for each PDGF. The protocol began with prepping the paraffin-embedded tissues. Tissues were fixed and sectioned previously, so first they were

deparaffinized in three xylene changes for 5 minutes each. A staining dish is filled two-thirds with 5 times used xylene for the first submersion. The slides with the tissue samples were loaded into the slide tray and lowered into the xylene. All submersions and washes used the same volume of solution, with the completely submerged in the solution. Following the first 5-minute submersion, the slide tray with the tissue samples was moved into a staining dish filled with 2-3 times used xylene for 5 minutes. Following the second 5-minute submersion, the slide tray was moved into another staining dish, filled with fresh xylene for 5 minutes. The xylene submersions all take place in the fume hood.

Following the last xylene submersion, the kidney samples were hydrated in ethanol washes. From the last xylene submersion, the slides were moved into a staining dish with 100% ethanol for 15 minutes. Following this 15-minute ethanol wash, another staining dish is filled with 100% ethanol for a second 15-minute wash. Next, two 90% ethanol washes were performed for 15 minutes each, following the same procedures. During these hydrations, the kidney samples were observed to make sure they were being hydrated but not removed from the slide.

Following hydration in ethanol, the tissue samples were washed in DI water for 1 minute by submerging them. During this wash, the slide tray was shaken up and down to ensure full rinsing of ethanol.

The slide tray was then removed from the DI water wash, and the tissue samples were tapped off. The slide was then held at a 45° angle with the longer end contacting the paper towel. The kidney slide was then tapped 5-7 times on the paper towel. The remaining water was removed by carefully dabbing around the kidney with a Kimwipe.

Next, a blue wax pencil was used to circle the kidney. This wax border is drawn to keep solutions localized on the kidney for incubation. The wax border may result in some blue coloring being present in the resulting slides, which can be attributed to smearing of the wax border.

Tissue samples were then incubated with 40uL blocking serum for 1 hour at 4°C. UltraCruz Blocking Reagent sc-516214 was pipetted onto the kidneys within the wax border on each slide. The wax border holds the liquid over the kidney to prevent the serum from running off the slide. During this hour incubation period, the kidneys were placed in a plastic container with a lid. At the bottom of the container was a paper towel, moistened with DI water to keep the kidneys in a humid environment. The kidney samples themselves were elevated from the paper towel and placed spanning two pipette tips.

Following the incubation period, the blocking serum was removed. Again, the slides were tapped off over a paper towel.

After blocking serum removal, 40 µL of primary antibody at a 1:50 dilution in blocking serum was added to each kidney sample. The primary antibody is specific to the PDGF monomer, either PDGF-B sc-365805 or PDGF-D sc-137030. Only one primary antibody was used in each procedure. The primary antibody was not added to the negative control/secondary only kidney sample. The tissue samples were incubated overnight at 4°C with primary antibody in the same humid plastic container.

After the overnight incubation, the tissues were tapped off again. The space within the wax circle around the kidneys was also dabbed with a Kimwipe to absorb extra primary antibody. Next, the tissue samples were incubated for 120 minutes with 40µL of secondary antibody (m-IgG_K BP-HRP sc-516102) at a 1:25 dilution in blocking serum. This incubation was at 4°C in the same plastic container.

Next, the peroxidase substrate and chromogen mixture was prepared. SIGMAFAST 3,3'-Diaminobenzidine (DAB) tablets (D4293-50SET) stained PDGFs brown. DAB was mixed in a 30mL conical tube. The solution reacts with light, so the conical tube was first wrapped in aluminum foil. Then two tablets of DAB, one gold and one silver, were placed in the conical tube, then 3mL of Millipore water was added to the conical tube. The solution was vortexed for 5 minutes.

The kidney samples were then removed from the fridge in the plastic container. The slides were then tapped off again to remove all secondary antibody. The lid of the plastic container was removed, with the kidney samples inside. The designated volume of 40 μ L of the chromogen mixture was added to each kidney. The lid was placed back on the container and the samples were incubated at room temperature for 15 minutes. Following the incubation period, the slides were tapped off again, then washed in DI water. Slides may have been counterstained in Ricca's Hematoxylin Stain Solution Cat# 3530-16 for 30 seconds, then washed with several changes of DI water.

Tissue samples were then dehydrated with ethanol washes. Two 3-minute washes were performed with 90% ethanol, then two 3-minute washes are performed with 100% ethanol. The tissue slides were then moved to a staining dish filled with xylene and removed individually for fixation. Following removal from the xylene dish, 2-4 drops of Permount was added to the circled kidney section of each slide, then a glass coverslip was placed, and the slide was allowed to dry overnight. The following day, slides were wiped with xylene to wash off any Permount and allow clear visualization.

As an additional control, some mouse kidney sections were treated only with hematoxylin. For this treatment, tissues were sectioned, deparaffinized, and hydrated the same way as for IHC. Instead of blocking, treating with antibodies, and adding DAB chromogen, these samples were

instead only counterstained with hematoxylin. They were then dehydrated through the same procedure as the full IHC treatment and visualized.

Slides were visualized under a light microscope using polarized light to view staining of PDGF-B or PDGF-D. Nuclei are stained blue and regions with PDGFs appear brown.

Visualizing and Assessing PDGF Presence

Following IHC, the slides were visualized under polarized light to view PDGF presence in glomeruli of *Colla2* deficient kidney sections. Stain should show specific region of kidneys and possibly the cell type affected.

Table 1. Mouse Identification Sheet.

ID	Genotype	Sex
B791	oim	F
B795	oim	F
B802	oim	F
B811	oim	F
B864	oim	F
B764	oim	M
B788	oim	M
B790	oim	M
B807	oim	M
B809	oim	M
B772	wt	F
B774	wt	F
B792	wt	F
B794	wt	F
B863	wt	F
B865	het	F
B769	wt	M
B771	wt	M
B805	het	M
B818	wt	M
B858	wt	M

VERIFYING DISEASE STATE AND LESION SCORES OF GENOTYPES

Table 2 shows the assigned lesion scores for each mouse kidney sample from PSR staining. Overall, all wildtype mouse kidneys had a lesion score of 0, both heterozygous mouse kidneys had lesion scores of 1, and *Colla2* deficient mouse kidneys had lesion scores of 2-4.

Figure 8 shows internal control vessels from PSR staining. All blood vessels contain type I collagen, so these can be used as an internal control to verify the PSR staining is effectively staining type I collagen red. An arrowhead points to each blood vessel in Figure 8. In Figure 8A, the glomeruli do not show much staining because it is a wildtype mouse with little type I collagen in the glomeruli, but the vessel on the left of the image (with an arrowhead) shows bright red staining from the presence of type I collagen. In Figure 8B, the glomeruli do stain bright red, as does the vessel in the bottom right of the image marked by the arrowhead. This mouse is *Colla2* deficient, and thus has an excess of type I collagen in the glomeruli causing them to stain bright red. Similarly, Figure 8C shows bright red glomeruli and a bright red vessel across the middle of the image. This mouse is also *Colla2* deficient and has excess type I collagen in the glomeruli. The bright red staining of the vessels in all three images, along with the matching staining of glomeruli in relationship to their genotype verifies that PSR staining was successful in showing type I collagen presence in the mouse kidney sections.

Figure 9 shows representative images of lesion scores from PSR staining. In Figure 9A, this wildtype mouse's glomeruli appear circular and are a uniform pink color. Urinary space of each glomerulus is unobstructed leaving room for accumulating urine during filtration. Because all the glomeruli in these kidneys are unaffected and there are no areas of extra collagen accumulation, these kidneys are scored a 0, meaning no disease is present. In Figure 9B, some of

the glomeruli from this heterozygous mouse have areas of extra red coloration, which is excess type I collagen accumulating in the mesangium of glomeruli. Many glomeruli in these images still appear unaffected with their circular shape, uniform pink color, and open urinary spaces. Because less than 25% of total glomerular area is affected and there are unaffected glomeruli present, these kidneys are scored at 1, meaning there is slight lesions showing minimal disease. In Figure 9C, this *Col2a2* deficient mouse has all glomeruli showing some amount of extra red coloration. Some glomeruli are distended, and urinary spaces are partially blocked. Because 25-50% of glomerular area is affected, this mouse kidney is scored a 2, meaning there are moderate lesions showing disease. In Figure 9D, this *Col2a2* deficient mouse has all glomeruli showing significant red coloration. All glomeruli are partially distended, and most urinary spaces are blocked. Because 50-75% of glomerular area is affected, these mouse kidneys are scored 3, meaning there are moderate lesions showing disease. In Figure 9E, this *Col2a2* deficient mouse has all glomeruli showing significant red coloration. All glomeruli are distended with urinary spaces blocked. Nearly the entire glomerular area shows bright red coloration, indicating significant collagen deposition. Because greater than 75% of glomerular area is affected, these kidneys are scored 4, meaning severe lesions are present.

Due to the homozygous *Colla2* deficient mice being unable to produce healthy, heterotrimeric type I collagen, it is expected that they will show significant disease from the type I collagen accumulation in the mesangia of glomeruli. All homozygous *Colla2* deficient mice showed lesion scores 2-4. Because heterozygous *Colla2* deficient mice have one allele for the homotrimeric form of type I collagen, they could show disease, but it was expected to be lesser than homozygous mice, which was the case. Both heterozygote mice had lesion scores of 1. As

expected, all wildtype mice had lesion scores of 0. These results further justify that Type I Collagen Glomerulopathy is a suitable model for renal fibrosis and glomerulopathy.

Figure 10 shows a comparison of wildtype and *Colla2* deficient mouse kidney sections with extra digital zoom into the glomeruli. Figure 10A shows a wildtype mouse kidney section, with pink, even glomeruli that have open, white urinary spaces. The glomeruli are also circular and average size. Figure 10B shows a *Colla2* deficient mouse kidney section. These glomeruli have patches of bright red staining, and swelling of the glomeruli which obstructs portions of the urinary space (denoted by asterisks). The glomeruli are also irregularly shaped, with one being larger than average size. Figure 10C shows a *Colla2* deficient mouse kidney section with mostly bright red glomeruli. The urinary spaces are mostly closed off due to swelling of the glomeruli. These glomeruli are also misshapen, with holes and very large size (over 100 μ m). Glomeruli appear brighter red at higher lesion scores due to more collagen deposition. Microscope images of lesion scores of 4 (Figure 9E and 10C) appear darker overall to accommodate the bright red coloration and prevent oversaturation. Glomeruli also appear larger at higher lesion scores, with all glomeruli in Figure 8A and 8B being less than 100 μ m, but many glomeruli at higher lesion scores being greater than 100 μ m.

Many glomeruli in diseased kidneys are larger than in wildtype kidneys. It is known that functional glomeruli within a diseased kidney will undergo hypertrophy to maintain GFR, so the larger glomeruli in the diseased kidneys could still be functional.²⁴ Glomeruli will also change size in healthy conditions due to other factors that increase demand for blood filtration.²⁵ However, the larger diseased glomeruli may also stretch to such diameters because of the significant collagen deposition in the mesangial, causing distension past the urinary space. An average mouse glomerulus should have a diameter of 70 μ m at the center of the sphere.^{25, 26} Many

of the diseased glomeruli have a diameter of over 100 μ m. This large increase in diameter and significant level of distension is likely not from the slight atrophy of increasing GFR, but rather the deposition of collagen in the mesangium of the diseased glomeruli. However, diameter of the glomerular section can be misleading, because glomeruli are circular; a section closer to the center of a glomerulus will show a larger glomerulus in section. Additionally, a section near the top of the sphere will be smaller due to a smaller diameter at that point. Because of these limitations to glomerular measurements via sectioning, this topic needs more exploration to prove the cause of the increase in glomerular diameter and the degree of the increase.

Table 2. Assigned Lesion Scores Following PSR.

ID	Genotype	Sex	Lesion Score
B722	wt	F	0
B774	wt	F	0
B792	wt	F	0
B794	wt	F	0
B863	wt	F	0
B769	wt	M	0
B771	wt	M	0
B818	wt	M	0
B858	wt	M	0
B865	het	F	1
B805	het	M	1
B791	<i>Colla2</i> Def	F	3
B795	<i>Colla2</i> Def	F	3
B802	<i>Colla2</i> Def	F	4
B811	<i>Colla2</i> Def	F	3
B864	<i>Colla2</i> Def	F	4
B764	<i>Colla2</i> Def	M	2
B788	<i>Colla2</i> Def	M	4
B790	<i>Colla2</i> Def	M	4
B807	<i>Colla2</i> Def	M	4
B809	<i>Colla2</i> Def	M	4

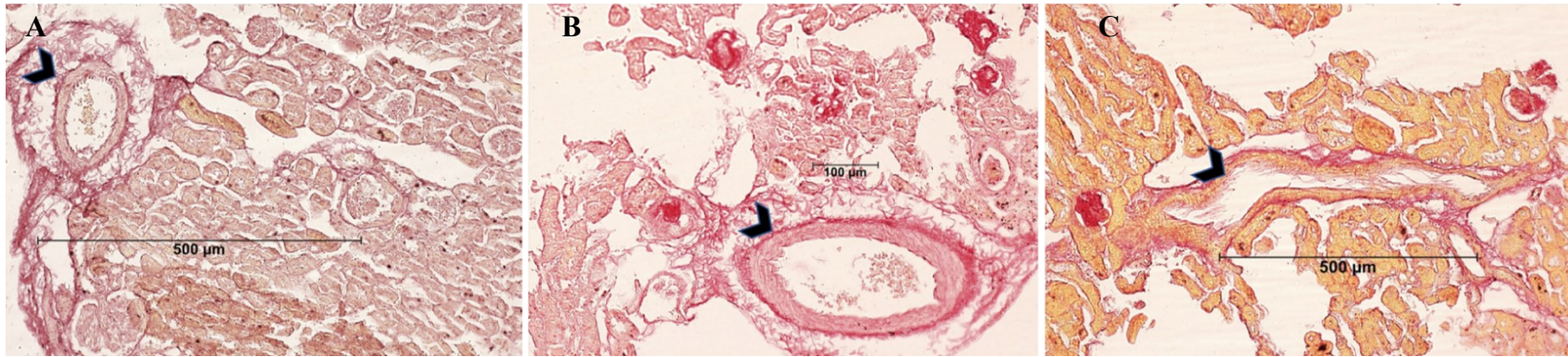


Figure 8. PSR Internal Control Vessels. All images in this figure were stained with PSR protocol. Arrow heads indicate vessels. A) Wildtype Male B818 PSR stained kidney section with lesion score of 0. Microscope image at 10x, scale of 500 μ m B) *Colla2* Deficient Female B791 PSR stained section with lesion score of 3. Microscope at 10x with digital zoom, scale of 100 μ m. C) *Colla2* Deficient Male B790 PSR stained kidney section with lesion score of 4. Microscope image at 10x, scale of 500 μ m.

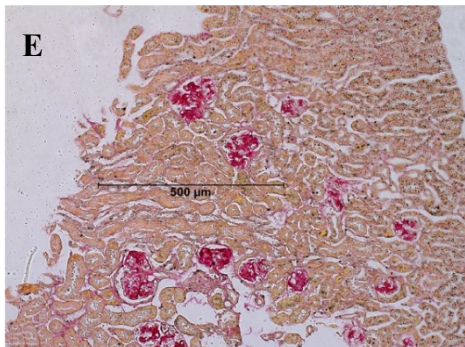
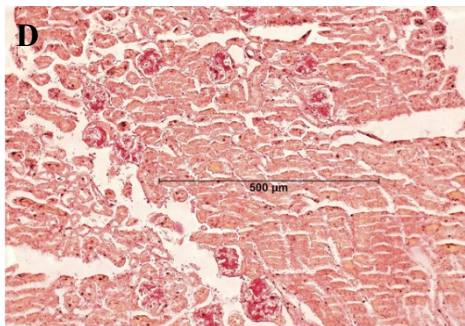
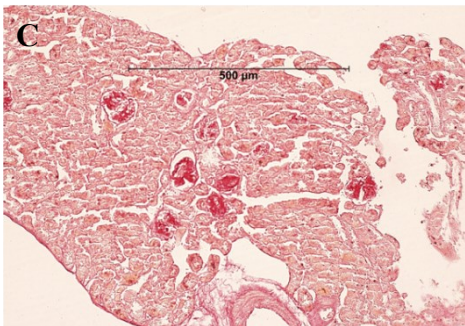
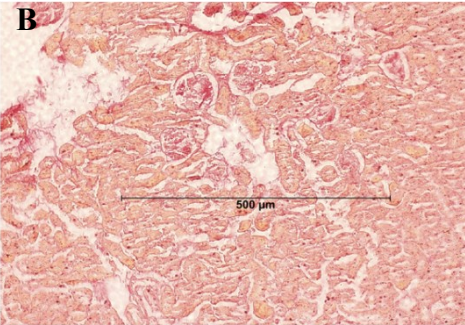
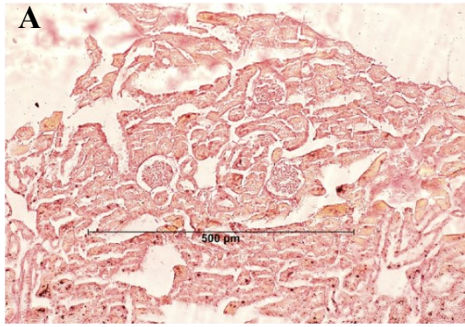


Figure 9. PSR Lesion Score Representative Images. All microscope images in this figure were stained with PSR protocol and imaged at 10x with digital zoom and 500 μ m scale. A) Wildtype Female B772 mouse kidney section with lesion score 0. B) Heterozygous Female B865 mouse kidney section with lesion score of 1. C) *Colla2* deficient Male B764 mouse kidney section with lesion score of 2. D) *Colla2* deficient Female B791 mouse kidney section with lesion score of 3. E) *Colla2* deficient Male B809 mouse kidney section with lesion score of 4. The brightness of kidney sections with a lesion score of 4 must be lowered to prevent oversaturation of the image with the bright red staining.

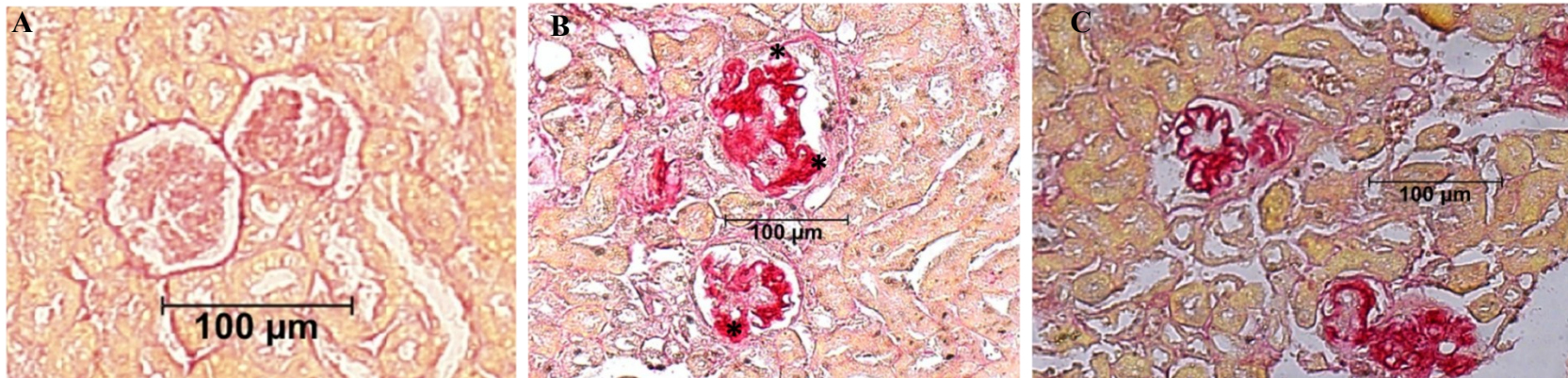


Figure 10. PSR Comparison. All microscope images in this figure were stained with PSR protocol and imaged at 10x with digital zoom and 100 μ m scale. A) Wildtype Female B774 mouse kidney section with lesion score of 0. B) *Colla2* deficient Female B802 mouse kidney section with lesion score of 3. Asterisks denote affected glomeruli and urinary space. C) *Colla2* deficient Female B795 mouse kidney section with lesion score of 4. The brightness of kidney sections with a lesion score of 4 must be lowered to prevent oversaturation of the image with the bright red staining.

DETERMINING DIFFERENTIAL PRESENCE OF PDGF-B AND PDGF-D

Figure 11 shows IHC controls. *Colla2* deficient mouse kidney sections were stained with hematoxylin only for Figure 11A to determine the appearance of glomeruli, marked with an asterisk. These glomeruli appear large, distended, grey, and with closed-off urinary spaces. This appearance of these glomeruli further verifies the disease state of the *Colla2* deficient mice, in that they have glomerulopathy from deposition in mesangia. The appearance of the diseased glomeruli and the baseline color helps in determining PDGF presence in mouse kidney sections that underwent IHC. Figure 11B shows *Colla2* deficient mouse kidney sections with the secondary-only IHC treatment. The glomeruli in this image should look the same as the hematoxylin-only image, because neither have the primary antibody to bind the conjugate for DAB. Both do appear without any brown coloration from PDGF, which verifies the IHC protocol was performed without contamination. The glomeruli in Figure 11B also appear large, distended, grey, and with closed-off urinary spaces, as shown by the asterisks marking glomeruli. Figure 11C shows wildtype secondary-only treatment, which also shows no brown staining, as expected. Furthermore, these glomeruli appear healthy, with smaller size, purple color, contained circles, and open urinary spaces, as marked by the pluses on example glomeruli. With these controls, the disease state was verified, the diseased glomeruli were categorized, and the IHC procedure was shown to be successful without contamination.

Figure 12 shows results of PDGF-B IHC on mouse kidney samples. This procedure further verified the disease state shown in the PSR results. In Figure 12A, the wildtype mouse kidney section shows healthy, circular glomeruli with defined and unobstructed urinary spaces. Additionally, this figure shows scattered brown coloration around the section. This coloration is

considered a basal level of expression in a wildtype tissue without damage, as PDGFs are involved in many healthy processes such as blood vessel formation. Furthermore, the PDGF-B being stained in wildtype mouse kidney samples could be unbound to receptors and not end up inducing receptor response. Because the PSR results and IHC results of wildtype tissues all show healthy glomeruli, the minimal PDGF-B staining in Figure 12A can be considered the basal level of PDGF-B protein expression without any alteration from disease. In Figure 12B, the heterozygous mouse kidney section shows healthy glomeruli, although they are slightly larger and have some obstruction of urinary spaces. This figure also shows slightly more brown coloration, still scattered around the kidney. Heterozygous mice had minor lesions, so more PDGF presence is expected to generate collagen deposition. Figures 12C and 12D show diseased glomeruli, with large sizes, distension, holes, and closed off urinary spaces. These glomeruli match with the disease state and suggest collagen deposition has occurred. Furthermore, these mouse kidney sections show significant brown coloration in glomeruli, as marked by asterisks in the affected glomeruli. Also, Figure 12D shows brown coloration in the vessel, as marked by the arrowhead, which is expected due to the platelets present in vessels.

Figure 13 shows mouse kidney sections that were treated with IHC involving PDGF-D. As shown in Figure 13A and very similar to PDGF-B, wildtype mouse kidney sections showed some brown staining scattered around the kidneys. However, as shown in Figure 13B, heterozygous mouse kidney sections showed some brown staining with PDGF-D primarily around tubules, not glomeruli. Shown in Figures 13C and 13D, homozygous *Colla2* deficient mouse kidney sections showed considerable brown staining with PDGF-D around tubules with minimal staining in glomeruli, as shown by the tall arrows. The glomeruli in these *Colla2* mouse

kidney sections are distended with closed-off urinary spaces, which verifies the disease state in these sections as well.

Figure 14 shows zoomed in images of a small area of the mouse kidney sections. Figure 14A shows a section treated with IHC involving PDGF-B. As shown in this image, there is brown throughout the tissue, with considerable amounts glomeruli (marked by asterisks), tubules (marked by tall arrows), and the vessel (marked with arrowhead). The whole tissue in this image appears more brown than purple, due to the high amount of PDGF-B present. In Figure 14B, there is less overall brown coloration, due to less PDGF-D being present than PDGF-B in 14A. Additionally, there are considerable amounts of brown coloration in tubules (marked by tall arrows) and the vessel (marked with tall arrowhead), but not in glomeruli. The glomeruli in this image appear grey and purple instead of brown, indicating PDGF-D is not found in diseased glomeruli. These images are from mouse kidney sections of the same mouse, *Colla2* deficient female B791 with a lesion score of 3. This direct comparison shows a difference in PDGF isoform location and amount. PDGF-B is found in glomeruli and tubules, and in larger amounts overall. However, PDGF-D is found primarily in tubules, and in smaller amounts overall.

Overall, it PDGF-B seems to have more presence and area in all *Colla2* mouse kidney samples. This higher amount could be attributed to a few factors. PDGF-B is a more versatile protein in general, with affinity for PDGFR- α and PDGFR- β monomers (thus all three receptor dimers: $\alpha\alpha$, $\alpha\beta$, $\beta\beta$), while PDGF-D only has affinity for the PDGFR- β monomer (thus only one receptor dimer: $\beta\beta$). Also, PDGF-B is involved in two dimer protein forms PDGF-AB and PDGF-BB, whereas PDGF-D is only involved in producing PDGF-DD. Likely PDGF-B's versatility in receptor affinity and dimer formation makes more PDGF-B present in mouse kidney samples. Furthermore, PDGF-B were found in tubules and glomeruli of these samples,

which suggests cells in both of these locations produce PDGF-B. PDGF-D was found mostly in tubules, suggesting tubules make PDGF-D whereas cells in the glomeruli do not. The amount of PDGF monomers and receptors should be determined in the future via protein assays of mouse kidneys.

These results suggest that PDGF-B may contribute to collagen deposition caused by Type 1 Collagen Glomerulopathy, as the glomerulus is the tissue where Type I collagen is deposited. PDGF-B IHC samples specifically show more staining around glomeruli, which suggests that mesangial cells and podocytes produce more PDGF-B. However, PDGF-D IHC samples show mostly just staining in tubules, which suggests tubular epithelial cells produce more PDGF-D. Given that these are the same mouse samples, deposition and resulting lesions are present in all *Colla2* samples, these results suggest that PDGF-B contributes to inducing glomeruli and damage, and PDGF-D contributes to inducing tubular damage. Thus, PDGF-B is likely a better target for future research involving Type I Collagen Glomerulopathy and other sources of glomerulopathy.

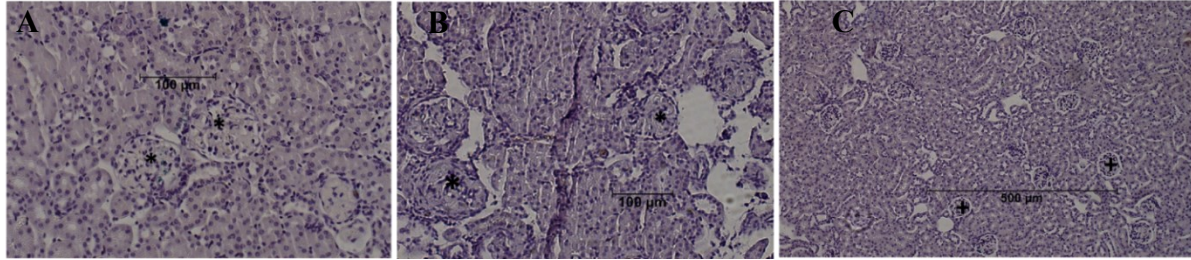


Figure 11. IHC Controls. All microscope images in this figure were counterstained with hematoxylin and imaged at 10x with digital zoom. Asterisks denote affected glomeruli, and pluses denote healthy glomeruli. A) *Colla2* Deficient Female B795 mouse kidney section without IHC treatment. This sample was only counterstained with hematoxylin. Image has 100 μ m scale. This mouse had a lesion score of 3 in PSR procedure. B) *Colla2* Deficient Female B811 mouse kidney section with secondary-only IHC treatment. Image has 100 μ m scale. This mouse had a lesion score of 3 in PSR procedure. C) Wildtype Female B863 mouse kidney section with secondary-only IHC treatment. Image has 500 μ m scale. This mouse had a lesion score of 0 in PSR procedure.

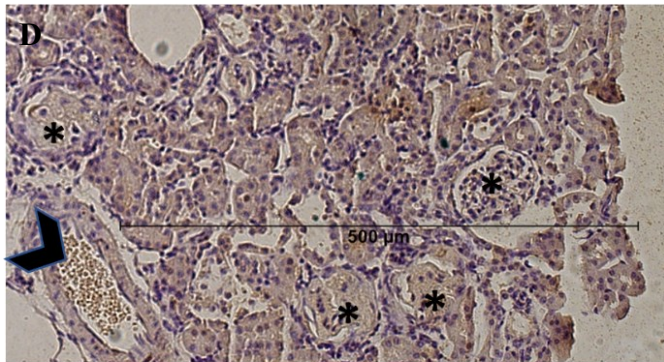
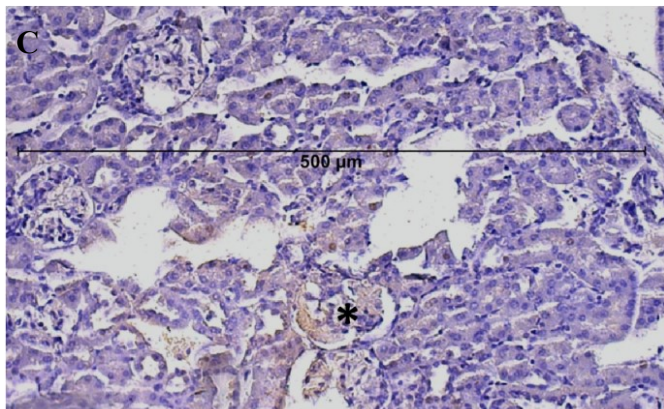
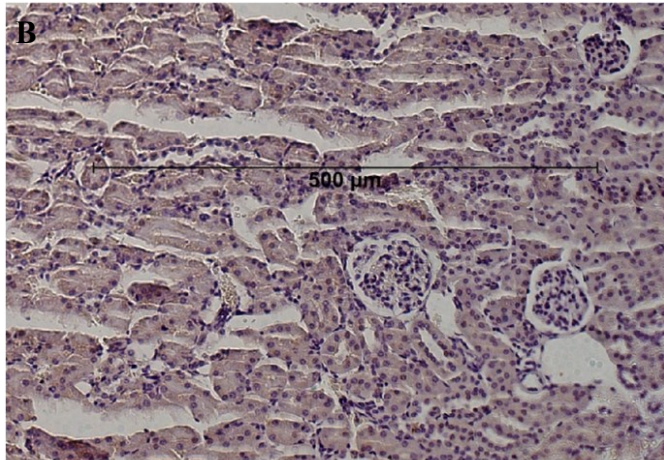
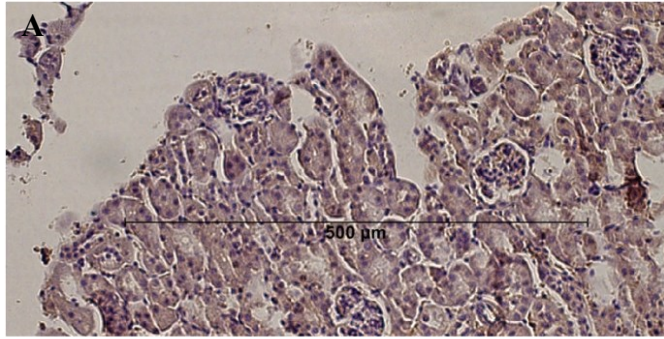


Figure 12. IHC with PDGF-B. All images in this figure were produced with IHC protocol with PDGF-B monomer and hematoxylin counterstain. Imaged at 10x with digital zoom and 500 μ m scale. A) Wildtype Male B769 mouse kidney section. This mouse had a lesion score of 0 in PSR procedure. B) Heterozygous Female B865 mouse kidney section. This mouse had a lesion score of 1 in PSR procedure. C) *Colla2* Deficient Female B811 mouse kidney section. This mouse had a lesion score of 3 in PSR procedure. Asterisk denotes affected glomerulus with brown coloration from PDGF-B presence. D) *Colla2* Deficient Female B791 mouse kidney section. Asterisk denotes affected glomeruli with PDGF-B presence. This mouse had a lesion score of 3 in PSR procedure. Arrowhead denotes vessel, which also shows PDGF-B presence.

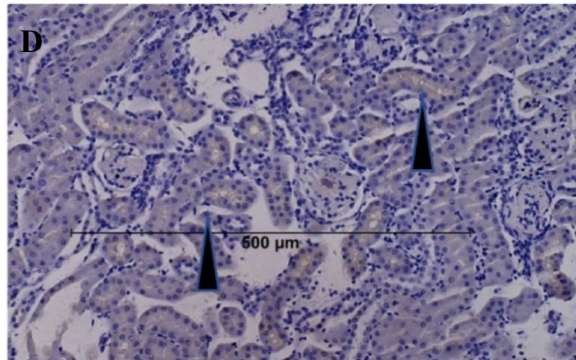
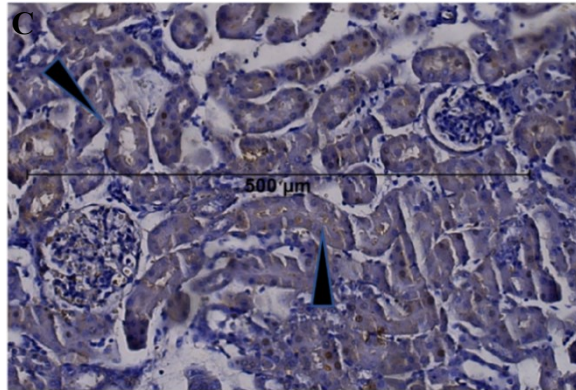
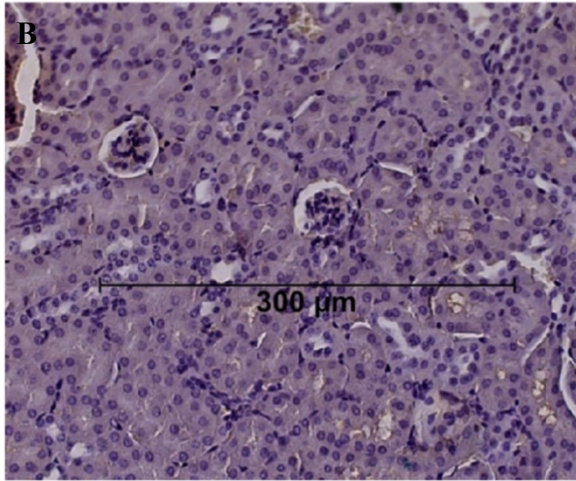
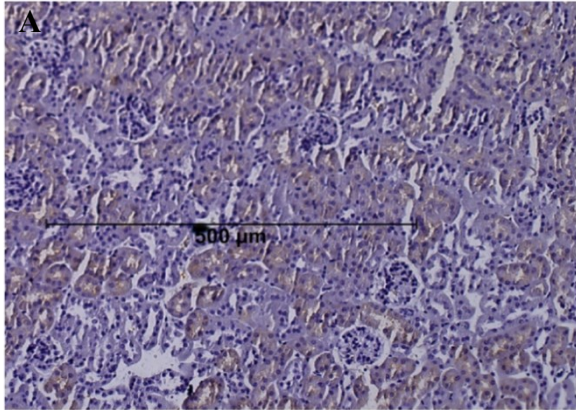


Figure 13. IHC with PDGF-D. All images in this figure were produced with IHC protocol with PDGF-D monomer and hematoxylin counterstain. Imaged at 10x with digital zoom. A) Wildtype Female B774 mouse kidney section with 500 μ m scale. This mouse had a lesion score of 0 in PSR procedure. B) Heterozygous Male B805 mouse kidney section with 300 μ m scale. This mouse had a lesion score of 1 in PSR procedure. C) *Colla2* Deficient Male mouse kidney section with 500 μ m scale. This mouse had a lesion score of 2 in PSR procedure. Tall arrows denote tubules with brown coloration. D) *Colla2* Deficient Male mouse kidney section with 500 μ m scale. This mouse had a lesion score of 4 in PSR procedure. Tall arrows denote tubules with brown coloration.

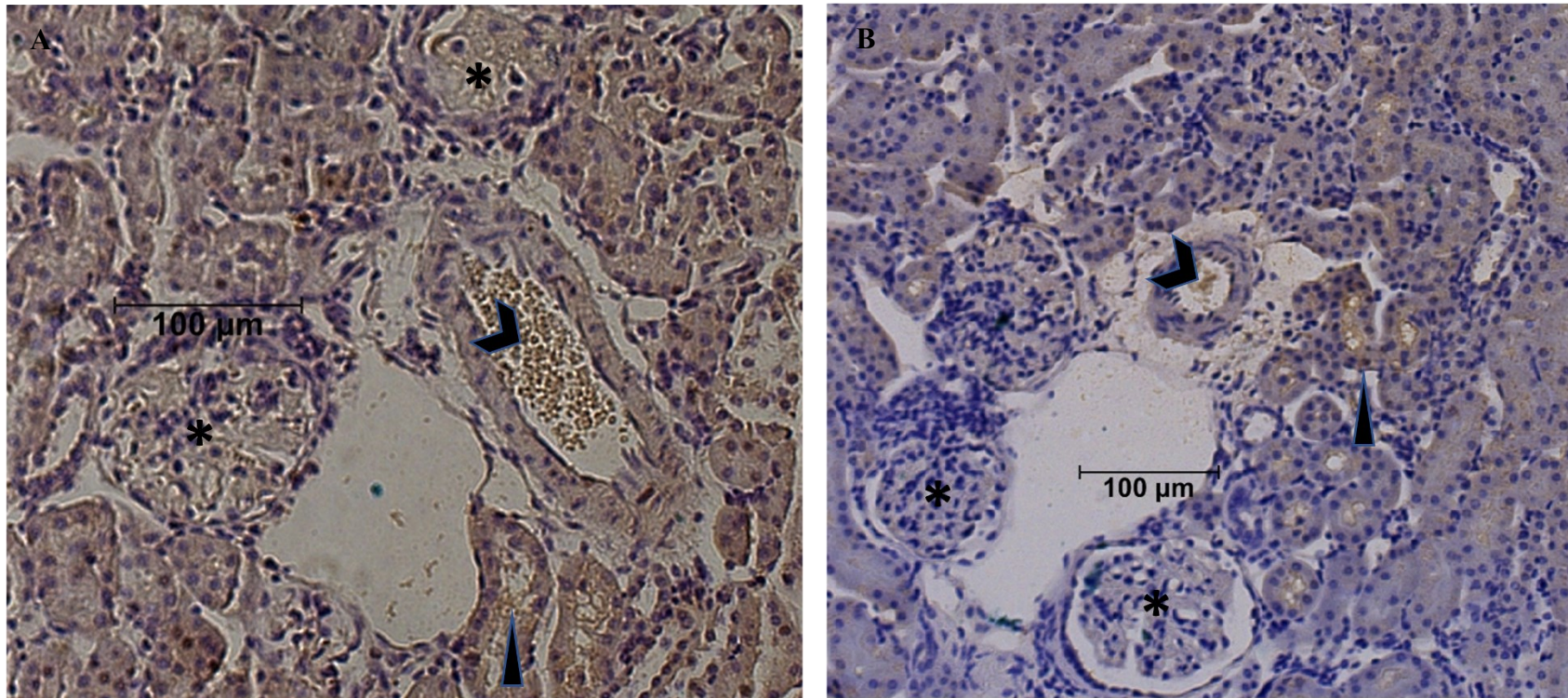


Figure 14. IHC Comparison Between PDGF Monomers. Both above images were produced with IHC protocol and hematoxylin counterstain. Imaged at 10x with digital zoom and 100μm scale. A) *Colla2* Deficient Female B791 mouse kidney section with IHC of PDGF-B. Mouse had a lesion score of 3. Asterisks denote glomeruli, tall arrows denote tubules, arrowhead denotes vessel. More brown coloration in this image is due to greater PDGF-B than PDGF-D in B. B) *Colla2* Deficient Female B791 mouse kidney section with IHC of PDGF-D. Mouse had a lesion score of 3. Asterisks denote glomeruli, tall arrows denote tubules, arrowhead denotes vessel.

DISCUSSION

PDGF-B shows staining both in glomeruli and in tubules, while PDGF-D mostly shows staining in tubules. Because glomerulopathy is the target, PDGF-B shows more potential for future treatments involving glomerulopathy as it binds more in glomeruli.

However, there are some limitations to this research and the verification of PDGFs in the mouse kidney tissues. One limitation is that the IHC procedures were not done with complete consistency. Although the same volumes, concentrations, and incubation times were used each time, some samples stained darker with hematoxylin, resulted in darker tissue sections, or had tearing from poor sectioning. These sources of artifact and inconsistent coloration means that PDGF quantities cannot be quantified, because background was not consistent between samples. In order to have consistent background with traditional IHC, sectioning, staining, and treatments would have to be made more uniform throughout to produce the exact same background in each sample such as through the use of automated IHC instrumentation.²⁷ Additionally, fluorescent IHC could be used with fluorescent secondary antibodies instead of chromogenic secondary antibodies.²⁸ This procedure would allow use of fluorescent microscopy to quantify antibody binding to each PDGF-isoform to produce relative expression levels between PDGFs and between genotypes.

Western blots could also be performed to determine the expression levels of each PDGF isoform and receptor isoform in wildtype, heterozygous, and *Colla2* deficient mice.²⁹ Depending on the part of the kidney assayed, expression of PDGFs and PDGFRs will likely be different. It would be valuable to do a western blot of the whole kidney, as well as western blot of glomerular

isolations. A whole kidney sample would be helpful in determining which PDGFs are involved in disease overall, but western blots of glomerular isolates would be more useful for studying progression of glomerulopathy. There are several methods for glomerular isolation including sieving or using Dynabeads.³⁰⁻³²

In addition to determining protein expression, it would be beneficial to determine PDGF RNA expression too, as they are the precursor to the PDGF protein. Future experiments could measure the expression of PDGF-B RNA via fluorescence in situ hybridization (FISH).³³ Interrupting PDGF-B function with siRNA could provide an additional avenue for slowing disease progression.³⁴

Furthermore, this research only involved finding PDGF isoforms in tissue, but PDGFs must interact with a receptor to trigger a response such as wound healing. Determining receptor quantities using western blots of mouse kidneys or glomerular isolations could determine if receptor isoform expression increases in disease states. Additionally, co-IHC with PDGF-B and the PDGFRs. PDGF-B monomer can bind either PDGFR monomers α or β , so future research could clarify which is being bound in glomeruli in Type I Collagen Glomerulopathy. It is expected that PDGF-B will bind PDGFR α , because PDGF-D was expressed in tubules and primarily binds PDGFR- β . PDGF-B can bind either receptor, so it could be binding the PDGFR- β receptors in the same region the PDGF-D were and the PDGFR- α in the glomeruli, as that was the other place PDGF-B were located in IHC results.

Another valuable future direction is determining whether PDGF-B initiation is involved only in Type I Collagen Glomerulopathy or kidney fibrosis largely. To explore this, IHC with PDGF-B could be performed on kidney sections from mice with a different source of kidney fibrosis, such as unilateral ureteral obstruction (UUO). This would involve either receiving

different extracted mouse kidneys from mice that have undergone UUO procedures compared to contralateral and healthy mouse kidneys, or housing live mice and performing the UUO. Similarly, drug-induced or sepsis induced fibrosis could be used to cause disease.¹⁴ These different models could verify that the presence of PDGF-B is similar in different sources of kidney fibrosis, not just the Type I Collagen Glomerulopathy disease.

Live models with PDGF-B knockdown could also be used. Knockouts for PDGFs, with a complete loss gene function, have been done in the past. PDGF-A knockout was lethal due to lung damage, and PDGF-B, PDGF-C, and PDGF-D knockouts reduced kidney fibrosis but resulting in structural changes.³⁵⁻³⁹ With these past examples and what is known about PDGFs importance to vascular development, knockdowns using miRNA are more viable for treatment.⁴⁰ In these mice, some could have the *Colla2* deficiency and others be otherwise healthy. Then the *Colla2* deficient PDGF-B knockdown mice could be compared to *Colla2* PDGF-B positive mice to see a difference in disease state. Furthermore, developmental changes with a lack of PDGF-B could be observed in the PDGF-B knockout mice without *Colla2* to distinguish the differences between PDGF-B function.

Overall, this research shows PDGF-B is found in higher prevalence in diseased glomeruli and tubules, and PDGF-D is found in higher prevalence in diseased tubules. This research was specific to the Type I Collagen Glomerulopathy model, so future research may focus on other models. Additionally, this research did not examine PDGFRs, so those will be studied in the future. Quantifications of PDGFs and PDGFRs can be done in the future to measure the difference in expression in disease states. Eventually knockdowns with PDGF-B will be done to hopefully limit disease progression without inhibiting development or function of kidneys and other vascular systems.

REFERENCES

1. Chronic Kidney Disease. 2021, September 03. <https://www.mayoclinic.org/diseases-conditions/chronic-kidney-disease/symptoms-causes/syc-20354521>.
2. Centers for Disease Control (CDC). Chronic Kidney Disease in the United States, 2021. 2021, March 04. <https://www.cdc.gov/kidneydisease/publications-resources/ckd-national-facts.html>.
3. Centers for Disease Control (CDC). Chronic Kidney Disease Basics. 2022, February, 28. <https://www.cdc.gov/kidneydisease/basics.html>.
4. Glick, A. D., Jacobson, H. R., & Haralson, M. A. (1992). Mesangial deposition of type I collagen in human glomerulosclerosis. *Human Pathology*, 23(12), 1373–1379.
5. Couser, W. G., & Johnson, R. J. (1994). Mechanisms of Progressive Renal Disease in Glomerulonephritis. *American Journal of Kidney Diseases*, 23(2), 193–198.
6. Biga, Lindsay M, et al. Anatomy and Physiology. Oregon State University. <https://open.oregonstate.education/aandp/>.
7. Ogobuiro I, Tuma F. Physiology, Renal. Updated 2021 Jul 26. In: StatPearls. Treasure Island (FL): StatPearls Publishing; 2022 Jan-. Available from: <https://www.ncbi.nlm.nih.gov/books/NBK538339/>
8. Al-Katib, S., Shetty, M., Jafri, S. M. A., & Jafri, S. Z. H. (2017). Radiologic assessment of native renal vasculature: A multimodality review. In *Radiographics* (Vol. 37, Issue 1, pp. 136–156). Radiological Society of North America Inc.
9. Richard Kitching, A., & Hutton, H. L. (2016). The players: Cells involved in glomerular disease. *Clinical Journal of the American Society of Nephrology*, 11(9), 1664–1674.
10. Merscher, S., Huwiler, A., Mccarthy, K., Nyström, J., Ebefors, K., & Bergwall, L. (2022). The Glomerulus According to the Mesangium. *Frontiers in Medicine | Www.Frontiersin.Org*, 1, 740527.
11. Schlöndorff, D., & Banas, B. (2009). The mesangial cell revisited: No cell is an island. In *Journal of the American Society of Nephrology* (Vol. 20, Issue 6, pp. 1179–1187).
12. Vaughan, M. R., & Quaggin, S. E. (2008). How do mesangial and endothelial cells form the glomerular tuft? In *Journal of the American Society of Nephrology* (Vol. 19, Issue 1, pp. 24–33).

13. Brodeur, A. C., Wirth, D. A., Franklin, C. L., Reneker, L. W., Miner, J. H., & Phillips, C. L. (2007). Type I collagen glomerulopathy: Postnatal collagen deposition follows glomerular maturation. *Kidney International*, 71(10), 985–993.
14. Bao, Y. W., Yuan, Y., Chen, J. H., & Lin, W. Q. (2018). Kidney disease models: tools to identify mechanisms and potential therapeutic targets. In *Zoological research* (Vol. 39, Issue 2, pp. 72–86). <https://doi.org/10.24272/j.issn.2095-8137.2017.055>
15. Phillips, C. L., Pfeiffer, B. J., Luger, A. M., & Franklin, C. L. (2002). GENETIC DISORDERS-DEVELOPMENT Novel collagen glomerulopathy in a homotrimeric type I collagen mouse (oim). In *Kidney International* (Vol. 62).
16. Roberts-Pilgrim, A. M., Makareeva, E., Myles, M. H., Besch-Williford, C. L., Brodeur, A. C., Walker, A. L., Leikin, S., Franklin, C. L., & Phillips, C. L. (2011). Deficient degradation of homotrimeric type I collagen, $\alpha 1(I) 3$ glomerulopathy in oim mice. *Molecular Genetics and Metabolism*, 104(3), 373–382.
17. Chang, S. W., Shefelbine, S. J., & Buehler, M. J. (2012). Structural and mechanical differences between collagen homo- and heterotrimers: Relevance for the molecular origin of brittle bone disease. *Biophysical Journal*, 102(3), 640–648.
18. Brodeur, A. C., Roberts-Pilgrim, A. M., Thompson, K. L., Franklin, C. L., & Phillips, C. L. (2017). Transforming growth factor- $\beta 1$ /Smad3- independent epithelial-mesenchymal transition in type I collagen glomerulopathy. *International Journal of Nephrology and Renovascular Disease*, 10, 251–259.
19. Fredriksson, L., Li, H., & Eriksson, U. (2004). The PDGF family: four gene products form five dimeric isoforms. *Cytokine & Growth Factor Reviews*, 15(4), 197–204.
20. Heldin CH. (2011) Platelet-Derived Growth Factor. In: Schwab M. (eds) *Encyclopedia of Cancer*. Springer, Berlin, Heidelberg.
21. Hudkins, K. L., Gilbertson, D. G., Carling, M., Taneda, S., Hughes, S. D., Holdren, M. S., Palmer, T. E., Topouzis, S., Haran, A. C., Feldhaus, A. L., & Alpers, C. E. (2004). Exogenous PDGF-D Is a Potent Mesangial Cell Mitogen and Causes a Severe Mesangial Proliferative Glomerulopathy. *Journal of the American Society of Nephrology*, 15(2), 286–298.
22. “Picrosirius Red Stain Kit.” Polysciences Inc. Catalog #24901. <https://www.polysciences.com/media/amasty/amfile/attach/hMyzQC7D3TZ2x3mJiHYgfv61gK8qiREX.pdf>.
23. “Immunoperoxidase Staining.” Santa Cruz Biotechnology. <https://www.scbt.com/resources/protocols/immunoperoxidase-staining>.

24. Jeansson, M., & Haraldsson, B. (2003). Glomerular size and charge selectivity in the mouse after exposure to glucosaminoglycan-degrading enzymes. *Journal of the American Society of Nephrology*, 14(7), 1756–1765.
25. Schlondorff, D. (1987). The glomerular mesangial cell: an expanding role for a specialized pericyte. *The FASEB Journal*, 1(4), 272–281.
26. Terasaki, M., Brunson, J. C., & Sardi, J. (2020). Analysis of the three dimensional structure of the kidney glomerulus capillary network. *Scientific Reports*, 10(1).
27. Prichard, J. W. (2014). Overview of automated immunohistochemistry. *Archives of Pathology and Laboratory Medicine*, 138(12), 1578–1582.
28. Zaqout, S., Becker, L. L., & Kaindl, A. M. (2020). Immunofluorescence Staining of Paraffin Sections Step by Step. *Frontiers in Neuroanatomy*, 14.
29. Hart, C. E., Seifert, R. A., Ross, R., & Bowen-Pope, D. F. (1987). Synthesis, phosphorylation, and degradation of multiple forms of the platelet-derived growth factor receptor studied using a monoclonal antibody. *Journal of Biological Chemistry*, 262(22), 10780–10785.
30. Rush, B. M., Small, S. A., Stolz, D. B., & Tan, R. J. (2018). An efficient sieving method to isolate intact glomeruli from adult rat kidney. *Journal of Visualized Experiments*, 2018(141).
31. Takemoto, M., Asker, N., Gerhardt, H., Lundkvist, A., Johansson, B. R., Saito, Y., & Betsholtz, C. (2002). A New Method for Large Scale Isolation of Kidney Glomeruli from Mice, 1799-1805.
32. Cui, S., Li, C., Ema, M., Weinstein, J., & Quaggin, S. E. (2005). Rapid isolation of glomeruli coupled with gene expression profiling identifies downstream targets in Pod1 knockout mice. *Journal of the American Society of Nephrology*, 16(11), 3247–3255.
33. Young, A. P., Jackson, D. J., & Wyeth, R. C. (2020). A technical review and guide to RNA fluorescence in situ hybridization. *PeerJ*, 8.
34. Han, H. (2018). RNA interference to knock down gene expression. In *Methods in Molecular Biology* (Vol. 1706, pp. 293–302). Humana Press Inc.
35. Boström, H., Willetts, K., Pekny, M., Lindahl, P., Kan Hedstrand, H., Pekna, M., Hellström, M., Gebre-Medhin, S., Schalling, M., Nilsson, M., Kurland, S., & Tö, J. (1996). PDGF-A Signaling Is a Critical Event in Lung Alveolar Myofibroblast Development and Alveogenesis PDGF receptor (PDGFR) and PDGFR. The current model of PDGF ligand-receptor interaction postulates tor (i.e., binding both A and B chains) (reviewed by Hel. In *Cell* (Vol. 85).

36. Levéen, P., Pekny, M., Gebre-Medhin, S., Swolin, B., Larsson, E., & Betsholtz, C. (1994). Mice deficient for PDGF B show renal, cardiovascular, and hematological abnormalities. *Genes & Development* 8:1875-1887.
37. Eitner, F., Bü, E., van Roeyen, C., Kunter, U., Rong, S., Seikrit, C., Villa, L., Boor, P., Fredriksson, L., Bäckström, G., Eriksson, U., Stman, A. O., Rgen Floege, J., & Ostendorf, T. (2008). PDGF-C Is a Proinflammatory Cytokine that Mediates Renal Interstitial Fibrosis.
38. Martin, I. v., Borkham-Kamphorst, E., Zok, S., van Roeyen, C. R. C., Eriksson, U., Boor, P., Hittatiya, K., Fischer, H. P., Wasmuth, H. E., Weiskirchen, R., Eitner, F., Floege, J., & Ostendorf, T. (2013). Platelet-derived growth factor (PDGF)-C neutralization reveals differential roles of PDGF receptors in liver and kidney fibrosis. *American Journal of Pathology*, 182(1), 107–117.
39. Buhl, E. M., Djurdjaj, S., Babickova, J., Klinkhammer, B. M., Folestad, E., Borkham-Kamphorst, E., Weiskirchen, R., Hudkins, K., Alpers, C. E., Eriksson, U., Floege, J., & Boor, P. (2016). The role of PDGF-D in healthy and fibrotic kidneys. *Kidney International*, 89(4), 848–861.
40. Knockdown Mice. 2022. Taconic. <https://www.taconic.com/genetically-engineered-animal-models/knockdown-mice/>.